Electronic Supplementary Information for

Chiral halogen and chalcogen bonding receptors for discrimination of stereo- and geometric dicarboxylate isomers in aqueous media

Jason Y. C. Lim,[a] Igor Marques,[b] Vítor Félix,[b] and Paul D. Beer[a]*

[a] Chemistry Research Laboratory, Department of Chemistry, University of Oxford, Mansfield Road, Oxford, OX1 3TA, UK.

[b] Department of Chemistry, CICECO – Aveiro Institute of Materials, University of Aveiro, 3810-193 Aveiro, 3810-193 Aveiro, Portugal.

E-mail: paul.beer@chem.ox.ac.uk

Contents

S1. Synthesis of Compounds

S1.1. General Information

All commercially available chemicals and solvents were used as received without further purification. All dry solvents were thoroughly degassed with N_2, dried through a Mbraun MPSP-800 column and used immediately. Water used was deionized and passed through a Milli-Q® Millipore machine for microfiltration. TBTA (tris(benzyltriazolemethyl)amine) was prepared according to reported procedures.[1] Chromatography was undertaken using silica gel (particle size: 40-63 μm) or preparative TLC plates (20 × 20 cm, 1 cm silica thickness).

NMR spectra were recorded on Bruker AVIII HD Nanobay 400 MHz, Bruker AVIII 500 MHz and Bruker AVIII 500 MHz (with ^{13}C cryoprobe) spectrometers. Low resolution electrospray ionization mass spectrometry (ESI-MS) was performed using the Waters Micromass LCT for characterization of compounds previously reported in the literature, and high resolution ESI-MS was recorded using Bruker microTOF spectrometer for novel compounds. Optical rotation data were measured on a Perkin-Elmer 241 polarimeter with a path length of 1 dm (using the 589 nm sodium D), with concentrations (c) reported in g/100 mL and temperatures reported in °C.

S1.2. Synthetic Procedures

The (*S*)-binaphthyl-2,2'-bis(azide) synthon was prepared from commercially-available enantiopure (*S*)-1,1′-binaphthyl-2,2′-diamine (BINAM) following a reported procedure.[2]

Neutral 2,2'-Iodotriazole XB Receptor Precursor 2.XB

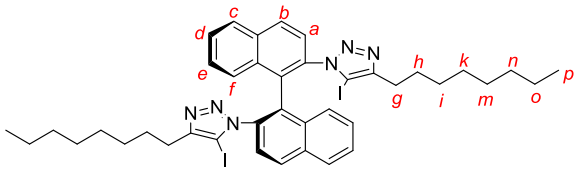

Sodium iodide (150 mg, 1.00 mmol) and copper(II) perchlorate hexahydrate (185 mg, 0.500 mmol) were mixed in THF/ acetonitrile 1:1 (3 mL) before DBU (36 mg, 0.24 mmol), TBTA (3.2 mg, 0.0060 mmol), 1-decyne (0.045 mL, 0.25 mmol) and the bis-azide synthon (40 mg, 0.12 mmol) were added portionwise sequentially. Stirring the reaction overnight resulted in a yellow slurry which was diluted with chloroform (30 mL) and washed successively with basic EDTA (2 x 10 mL), water (10 mL), brine (10 mL). After drying the reaction with $MgSO_4$ and solvent removal *in vacuo*, column chromatography (1 % methanol in dichloromethane) afforded the target compound as a pale yellow sticky solid (100 mg, 97 %).

^{1}H-NMR (400 MHz, $CDCl_3$) δ 8.00 (2H, d, ^3J = 8.8 Hz, H_a), 7.94 (2H, d, ^3J = 8.2 Hz, H_c), 7.52-7.56 (2H, m, H_b), 7.42 (2H, d, ^3J = 8.8 Hz, H_b), 7.36-7.39 (4H, m, H_e + H_f), 2.47-2.60 (4H, m, H_g), 1.54-1.61 (4H, m, H_h), 1.23-1.31 (20H, m, H_{i-o}), 0.88 (6H, t, ^3J = 6.9 Hz, H_p); **^{13}C-NMR** (100 MHz, $CDCl_3$) 151.3, 134.0, 132.7, 132.6, 130.1, 129.2, 128.0, 127.7, 127.0, 126.9, 124.0, 79.8, 31.5, 28.9, 28.8, 28.7, 28.2, 25.8, 22.3, 13.8; **MS** (ESI +ve) *m/z* 865.1945 ($[M + H]^+$, $C_{40}H_{47}N_6{}^{127}I_2$, calc. 865.1946).

Neutral 2,2'-Prototriazole HB Receptor Precursor 2.HB

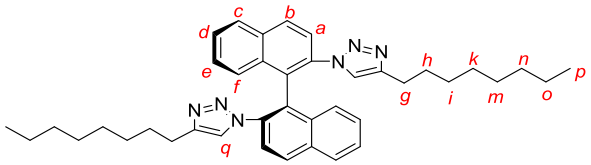

The bis-azide synthon (40 mg, 0.12 mmol), $[Cu(CH_3CN)_4]PF_6$ (18 mg, 0.048 mmol), TBTA (3.2 mg, 0.0060 mmol), 1-decyne (0.045 mL, 0.25 mmol) and DIPEA (0.062 mL, 0.36 mmol) were dissolved in degassed dichloromethane (3 mL) and left to react under ambient conditions overnight. The reaction was then partitioned between chloroform (20 mL) and basic EDTA solution (10 mL). The organic layer was separated and washed with basic EDTA (10 mL), water (10 mL) and brine (10 mL) before being dried with $MgSO_4$ and dried *in vacuo*. Silica gel column chromatography (2 % methanol in dichloromethane) afforded the target compound as a viscous yellow liquid (59 mg, 81 %).

^{1}H-NMR (400 MHz, $CDCl_3$) δ 8.07 (2H, d, ^3J = 8.3 Hz, H_a), 7.94 (2H, d, ^3J = 7.2 Hz, H_c), 7.73 (2H, d, ^3J = 8.3 Hz, H_b), 7.52 (2H, t, ^3J = 6.5 Hz, H_d), 7.36 (2H, t, ^3J = 6.5 Hz, H_e), 7.29 (2H, d, ^3J = 8.3 Hz, H_f), 7.23 (2H, s, H_q), 2.45 (4H, t, ^3J = 6.2 Hz, H_g), 1.18-1.33 (24H, m, $H_{h\text{-}o}$), 0.90 (6H, t, ^3J = 6.2 Hz, H_p); **^{13}C-NMR** (100 MHz, $CDCl_3$) δ 147.3, 134.7, 132.8, 131.9, 130.1, 128.0, 127.5, 127.3, 127.1, 125.8, 122.9, 121.9, 31.6, 28.9, 28.8, 28.7, 28.3, 24.8, 22.4, 13.8; **MS** (ESI +ve) *m/z* 613.4013 ($[M + H]^+$, $C_{40}H_{49}N_6$, calc. 613.4013).

Neutral 2,2'-Methylseleno-triazole ChB Receptor Precursor 2.ChB

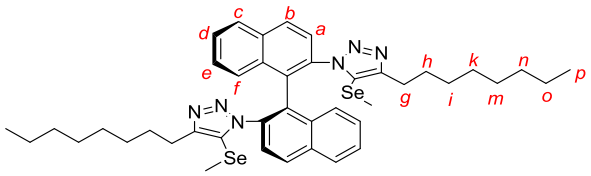

Warning: handle with care in fume cupboard due to malodourous nature of Se-containing volatiles formed in this reaction. All glassware in contact with the reaction was deodorized by soaking in bleach for at least 6 hours.

To a microwave vial containing powdered elemental selenium (71 mg, 0.90 mmol) was added a minimum amount of anhydrous THF to fully submerge the selenium. After sealing the vial under N_2, a 1.6 M solution of methyl lithium in hexane (0.56 mL, 0.90 mmol) was added with vigorous stirring at room temperature, whereupon a light brown slurry forms (sonicate if necessary to ensure homogeniety). The slurry was stirred for 30 minutes, before a solution of compound **2.XB** (65 mg, 0.075 mmol) in anhydrous THF (1.5 mL) was added portionwise to afford a dark brown solution, which was stirred at 100 ^oC in the dark for 2 days. Thereafter, the reaction was cooled to ambient temperature and iodomethane (0.1 mL) was added. The reaction was stirred vigorously for 30 minutes to form a light brown suspension before being poured into water (20 mL). The aqueous layer was extracted with chloroform (3 x 20 mL) and the combined organics were washed with brine (10 mL) and dried with $MgSO_4$. Solvent removal *in vacuo* and column chromatography (4 % methanol in dichloromethane) afforded the product as a pale yellow paste (45 mg, 75 %).

^{1}H-NMR (400 MHz, $CDCl_3$) δ 7.95 (2H, d, ^3J = 8.9 Hz, H_a), 7.84 (2H, d, ^3J = 8.1 Hz, H_c), 7.65 (2H, d, ^3J = 8.9 Hz, H_b), 7.30 (2H, t, ^3J = 7.6 Hz, H_d), 7.13 (2H, t, ^3J = 7.5 Hz, H_e), 6.98 (2H, d, ^3J = 8.4 Hz, H_f), 5.02-5.10 (4H, m, H_g), 4.04-4.17 (4H, m, H_h), 1.74 (4H, m, H_i),1.24-1.31 (20H, m, $H_{k\text{-}p}$), 0.85 (6H, t, ^3J = 6.8 Hz, H_q); **^{13}C-NMR** (100 MHz, $CDCl_3$) δ 152.0, 134.1, 134.0, 132.9, 130.7, 129.1, 128.5, 127.9, 127.1, 126.9, 124.3, 122.2, 31.9, 29.3, 29.2, 29.1, 25.8, 22.7, 14.1, 9.9; **MS** (ESI +ve) *m/z* 801.2657 ($[M + H]^+$, $C_{42}H_{53}N_6{}^{80}Se_2$, calc. 801.2657).

2,2'-Iodotriazolium (*S*)-Binaphthyl Dicationic XB Receptor 1.XB

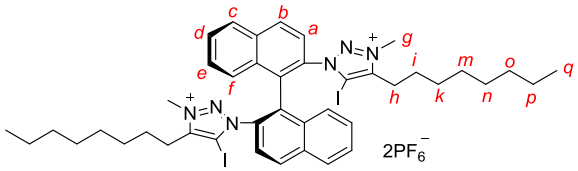

Neutral bis-iodotriazole precursor **2.XB** (62 mg, 0.072 mmol) was dissolved in dry dichloromethane (2 mL) and trimethyloxonium tetrafluoroborate (23 mg, 0.16 mmol) was added portionwise. The reaction was stirred overnight at room temperature before 1 drop of methanol was added and the solvent removed on a rotary. Purification by preparatory TLC (4 % methanol in dichloromethane) afforded the purified product, which was converted to its $2PF_6^-$ salt by repeated washing a chloroform solution (30 mL) of the purified compound with 0.1 M NH_4PF_6 (aq.) (8 x 10 mL) followed by water (2 x 10 mL). Drying the organic phase with $MgSO_4$ and solvent removal *in vacuo* gave the target compound as a pale yellow solid (60 mg, 71 %).

^{1}H-NMR (400 MHz, d_6-acetone) δ 8.54 (2H, d, ^3J = 8.9 Hz, H_a), 8.28 (2H, d, ^3J = 8.2 Hz, H_c), 8.04 (2H, d, ^3J = 8.9 Hz, H_b), 7.82 (2H, t, ^3J = 7.6 Hz, H_d), 7.65 (2H, t, ^3J = 7.6 Hz, H_e), 7.49 (2H, d, ^3J = 8.4 Hz, H_f), 4.05 (6H, s, H_g), 2.92 (4H, m, H_h), 1.49 (4H, m, H_i), 1.20-1.34 (20H, m, $H_{k\text{-}p}$), 0.89 (6H, t, ^3J = 7.2 Hz, H_q); **^{13}C-NMR** (100 MHz, d_6-acetone) δ 149.7, 135.2, 133.6, 132.8, 130.4, 130.0, 129.8, 129.7, 128.1, 124.9, 93.2, 39.2, 32.6, 29.8, 29.7, 27.8, 25.0, 23.4, 14.4; **^{19}F-NMR** (376 MHz, d_6-acetone) δ -72.7 (d, $^1J_{F\text{-}P}$ = 707 Hz); **^{31}P-NMR** (162 MHz, d_6-acetone) δ -144.4 (sep., $^1J_{P\text{-}F}$ = 707 Hz); **MS** (ESI +ve) *m/z* 447.1173 ($[M]^{2+}$, $C_{42}H_{52}N_6{}^{127}I_2$, calc. 447.1166); $[\alpha]_D^{25}$ +2.8 (c 0.10, acetone).

2,2'-Prototriazolium (*S*)-Binapthyl Dicationic HB Receptor 1.HB

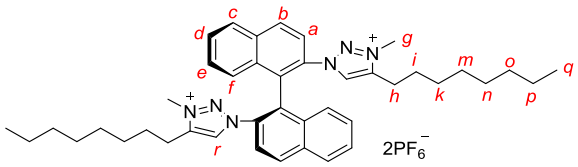

Identical methylation procedure as that for **1.XB**. Reagents: **4.7H** (27 mg, 0.044 mmol) with trimethyloxonium tetrafluoroborate (14 mg, 0.097 mmol) in dry dichloromethane (2 mL). Purification by preparatory TLC (4 % methanol in dichloromethane) and anion exchange by washing with 0.1 M NH_4PF_6 (aq.) as described for receptor **4.3I** gave the product as a pale yellow solid (29 mg, 71 %).

^{1}H-NMR (400 MHz, d_6-acetone) δ 8.65 (2H, s, H_r), 8.54 (2H, d, ^3J = 9.2 Hz, H_a), 8.29 (2H, d, ^3J = 8.2 Hz, H_c), 8.00 (2H, d, ^3J = 9.2 Hz, H_b), 7.81 (2H, t, ^3J = 7.6 Hz, H_d), 7.62 (2H, t, ^3J = 7.6 Hz, H_e), 7.42 (2H, d, ^3J = 8.6 Hz, H_f), 4.15 (6H, s, H_g), 2.81 (4H, m, H_h), 1.54 (4H, m, H_i), 1.19-1.31 (20H, m, $H_{k\text{-}p}$), 0.88 (6H, t, ^3J = 7.0 Hz, H_q); **^{13}C-NMR** (100 MHz, d_6-acetone) δ 146.3, 135.3, 133.6, 133.3, 133.2, 130.4, 130.2, 130.1, 130.0, 128.3, 127.4, 123.3, 38.4, 32.6, 29.8, 27.5, 23.5, 23.4, 14.4; **^{19}F-NMR** (376 MHz, d_6-acetone) δ -72.7 (d, $^1J_{F\text{-}P}$ = 707 Hz); **^{31}P-NMR** (162 MHz, d_6-acetone) δ -144.4 (sep., $^1J_{P\text{-}F}$ = 707 Hz); **MS** (ESI +ve) *m/z* 321.2199 ($[M]^{2+}$, $C_{42}H_{54}N_6$, calc. 321.2200); $[\alpha]_D^{25}$ -2.6 (c 0.10, acetone).

2,2'-Methylseleno-triazolium (*S*)-Binaphthyl Dicationic ChB Receptor 1.ChB

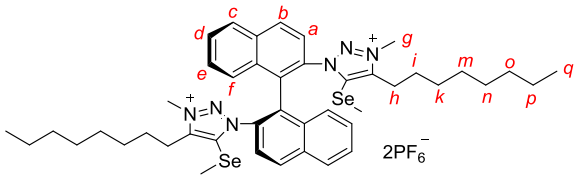

Identical methylation procedure as that for **1.XB**. Reagents: **4.7Se** (45 mg, 0.056 mmol) with trimethyloxonium tetrafluoroborate (18 mg, 0.12 mmol) in dry dichloromethane (1.5 mL). Crude product was found to be very clean and hence no further purification was necessary. Anion exchange by washing with 0.1 M NH_4PF_6 (aq.) as described for receptor **4.3I** yielded **4.3Se** as a pale yellow solid (55 mg, 87 %).

^{1}H-NMR (400 MHz, d_6-acetone) δ 8.49 (2H, d, ^{3}J = 8.8 Hz, H_a), 8.27 (2H, d, ^{3}J = 8.3 Hz, H_c), 7.95 (2H, d, ^{3}J = 8.8 Hz, H_b), 7.81 (2H, t, ^{3}J = 7.6 Hz, H_d), 7.63 (2H, t, ^{3}J = 7.6 Hz, H_e), 7.49 (2H, d, ^{3}J = 8.3 Hz, H_f), 4.08 (6H, s, H_g), 2.94 (4H, t, ^{3}J = 7.9 Hz, H_h), 2.52 (6H, s, SeCH_3), 1.48 (4H, m, H_i), 1.16-1.33 (20H, m, H_{k-p}), 0.89 (6H, t, ^{3}J = 7.0 Hz, H_q); **^{13}C-NMR** (100 MHz, d_6-acetone) δ 150.1, 135.4, 133.9, 132.8, 132.7, 132.0, 130.4, 130.2, 130.1, 129.9, 127.9, 124.9, 39.2, 32.8, 30.0, 29.9, 28.2, 24.6, 23.5, 14.6, 12.2; **^{19}F-NMR** (376 MHz, d_6-acetone) δ -72.7 (d, $^{1}J_{F-P}$ = 707 Hz); **^{31}P-NMR** (162 MHz, d_6-acetone) δ -144.4 (sep., $^{1}J_{P-F}$ = 707 Hz); **^{77}Se-NMR** (95 MHz, d_6-acetone) δ 105.0; **MS** (ESI +ve) *m/z* 415.1540 ($[M]^{2+}$, $C_{44}H_{58}N_6{}^{80}Se_2$, calc. 415.1521); $[\alpha]_D^{25}$ +4.4 (c 0.10, acetone).

Synthesis of tetrabutylammonium salts of dicarboxylates

Typical procedure:

To a chilled solution of the neutral bis-acid (anion precursor) (1.0 eqv) in water/THF 10:1 (*v/v*) at 0 ^{o}C was added a methanolic solution of tetrabutylammonium (TBA) hydroxide (2.0 eqv) over 5 minutes. The resulting reaction was allowed to warm up to ambient temperature and stirred for 30 mins. The TBA salt was obtained by removal of solvent *in vacuo* and leaving the salt to dry under high-vacuum for at least 3 days. The chiral dicarboxylate salts (tartrate and *N*Boc-glutamate) were stored in a vacuum dessicator with P_2O_5 dessicant at -20 ^{o}C to minimize racemization, while the geometric isomers (maleate/ fumarate, benzene dicarboxylates) were stored in a vacuum dessicator over P_2O_5 at ambient temperature.

S2. Spectral Characterization of Receptor Compounds

Receptor **1.XB**

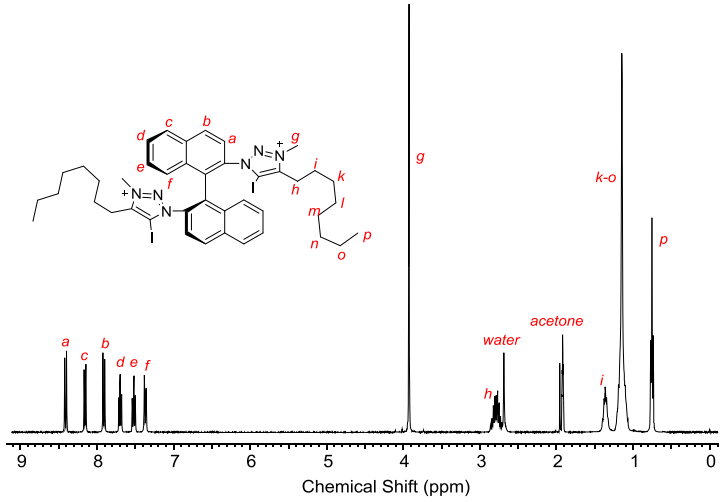

Fig. S2-1. ^{1}H NMR spectrum of receptor **1.XB** (400 MHz, d_6-acetone).

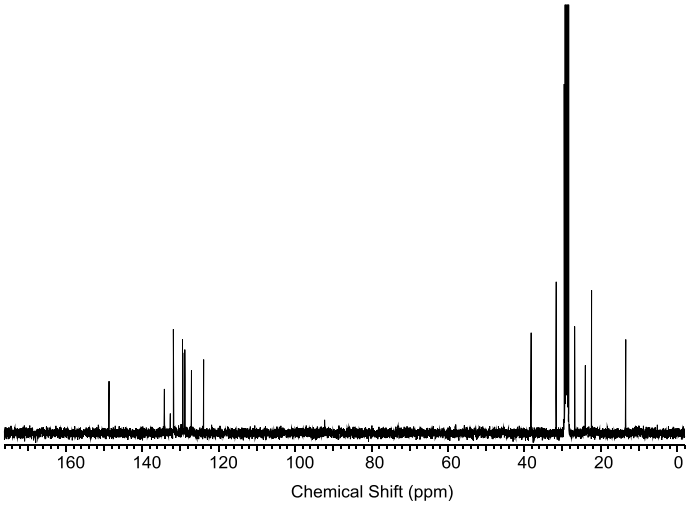

Fig. S2-2. ^{13}C-NMR of receptor **1.XB** (100 MHz, d_6-acetone).

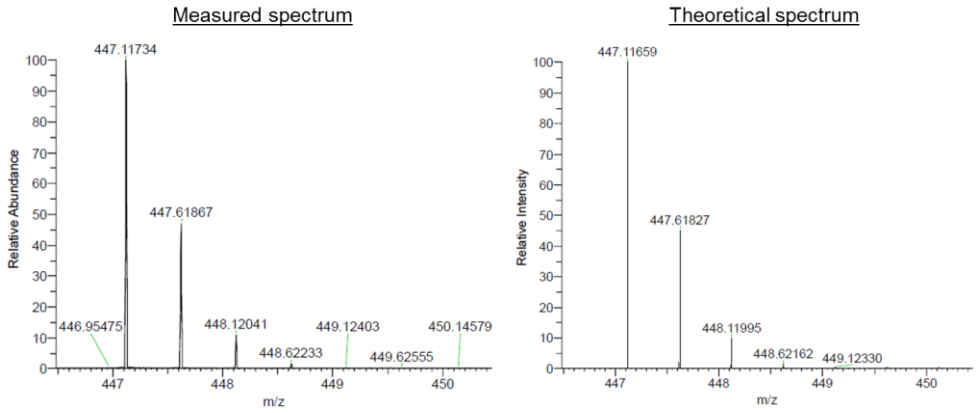

Fig S2-3. High-resolution ESI mass spectrum of receptor **1.XB** (left) and its theoretical calculated spectrum (right).

Receptor **1.HB**

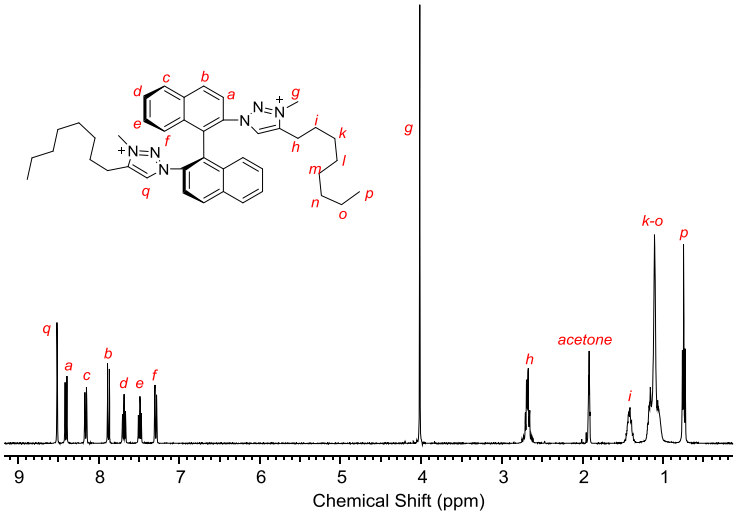

Fig. S2-4. ^{1}H NMR spectrum of receptor **1.HB** (400 MHz, d_6-acetone).

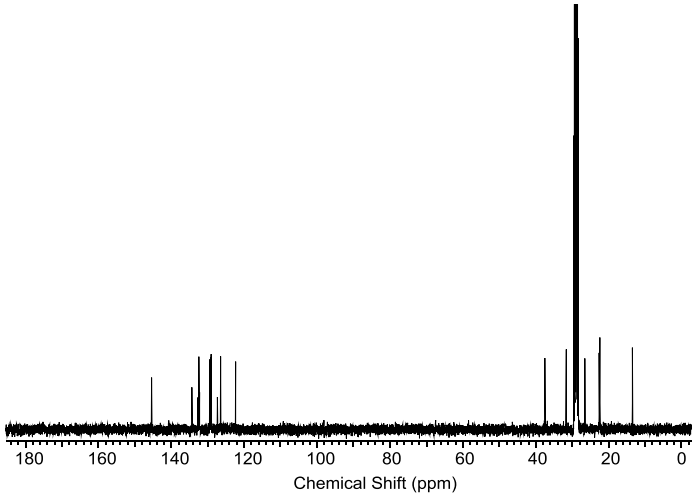

Fig. S2-5. ^{13}C-NMR of receptor **1.HB** (100 MHz, d_6-acetone).

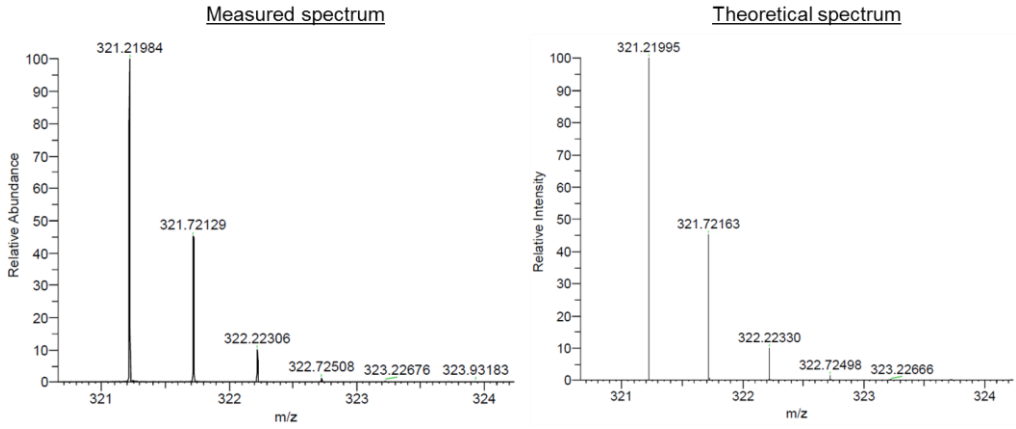

Fig S2-6. High-resolution ESI mass spectrum of receptor **1.HB** (left) and its theoretical calculated spectrum (right).

Receptor **1.ChB**

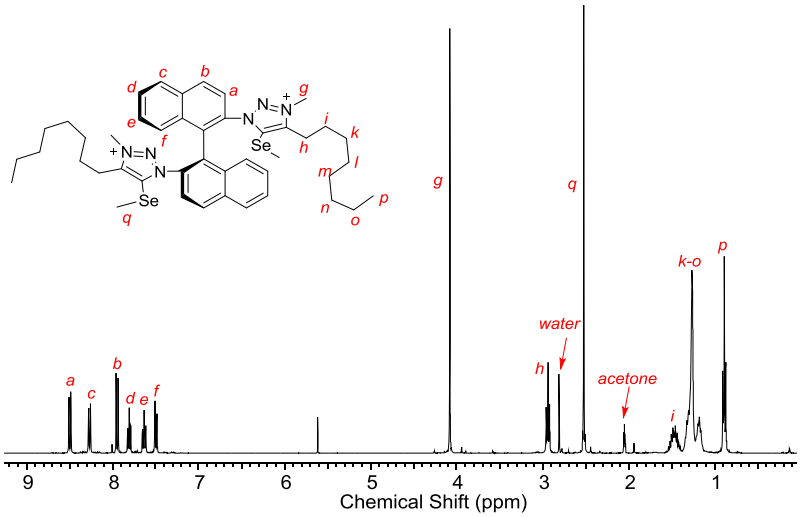

Fig. S2-7. ^{1}H NMR spectrum of receptor **1.ChB** (400 MHz, d_6-acetone).

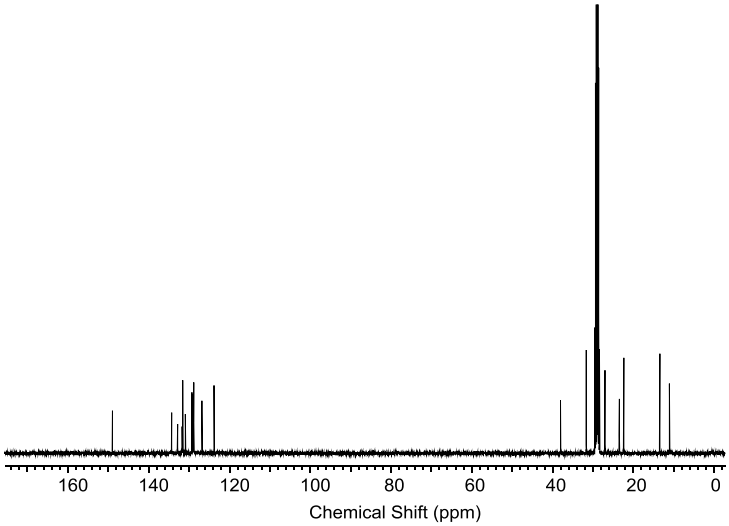

Fig. S2-8. ^{13}C-NMR of receptor **1.ChB** (100 MHz, d_6-acetone).

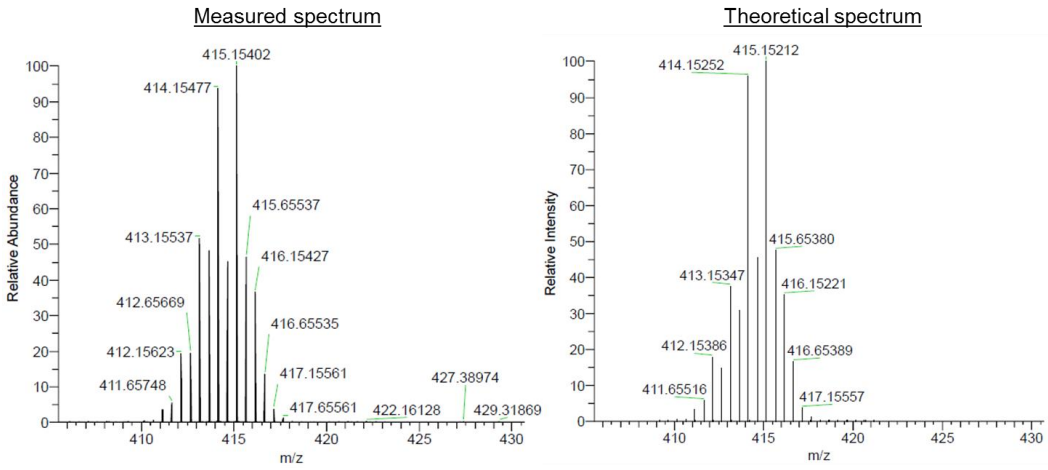

Fig S2-9. High-resolution ESI mass spectrum of receptor **1.ChB** (left) and its theoretical calculated spectrum (right).

S3. ^{1}H NMR Anion binding studies

General procedure

^{1}H NMR titration experiments were performed on a Bruker AVIII 500 MHz spectrometer. In a typical experiment, a solution of the appropriate tetrabutylammonium (TBA) salt in d_6-acetone/ D_2O 85: 15 *v/v* was added to a solution of the receptor molecule at 298 K with the same solvent combination. Both TBA salt and receptor were dissolved in the same solvent. TBA was chosen as the counter-cation due to its non-coordinating nature. A 0.05 M solution of the dicarboxylate salt was added to 0.50 mL of a 1.0 mM solution of receptor, where 1.0 equivalent of salt added corresponds to 10.0 µL of the salt solution. 19 data points corresponding to 0.0, 0.2, 0.4, 0.6, 0.8, 1.0, 1.2, 1.4, 1.6, 1.8, 2.0, 2.5, 3.0, 4.0, 5.0, 7.0, 10.0, 15.0 and 20.0 equivalents of added guest anion were obtained.

The binding of anions with all receptors were found to be fast on the NMR timescale. The values of the observed chemical shift at every concentration of host and anion were entered into the BindFit website[3] for every titration point. From initial estimates made of the binding constants and limiting chemical shifts, these parameters were refined using non-linear least-squares analyses to obtain the best fit between empirical and calculated chemical shifts based on the most appropriate host-guest binding model, which was selected based on the quality of fit and residual analysis from the data fitting. In almost all cases (see Table S3-1), a host-guest 1:2 binding model was the most appropriate.

For the following binding isotherms, empirical data points are represented by filled dots, while continuous lines represent the calculated binding curves. The binding isotherms obtained for the (*S*)-enantiomers of the chiral anions are represented in black, while those for the (*R*)-enantiomers are shown in red.

Receptor 1.XB

Tartrate Enantiomers

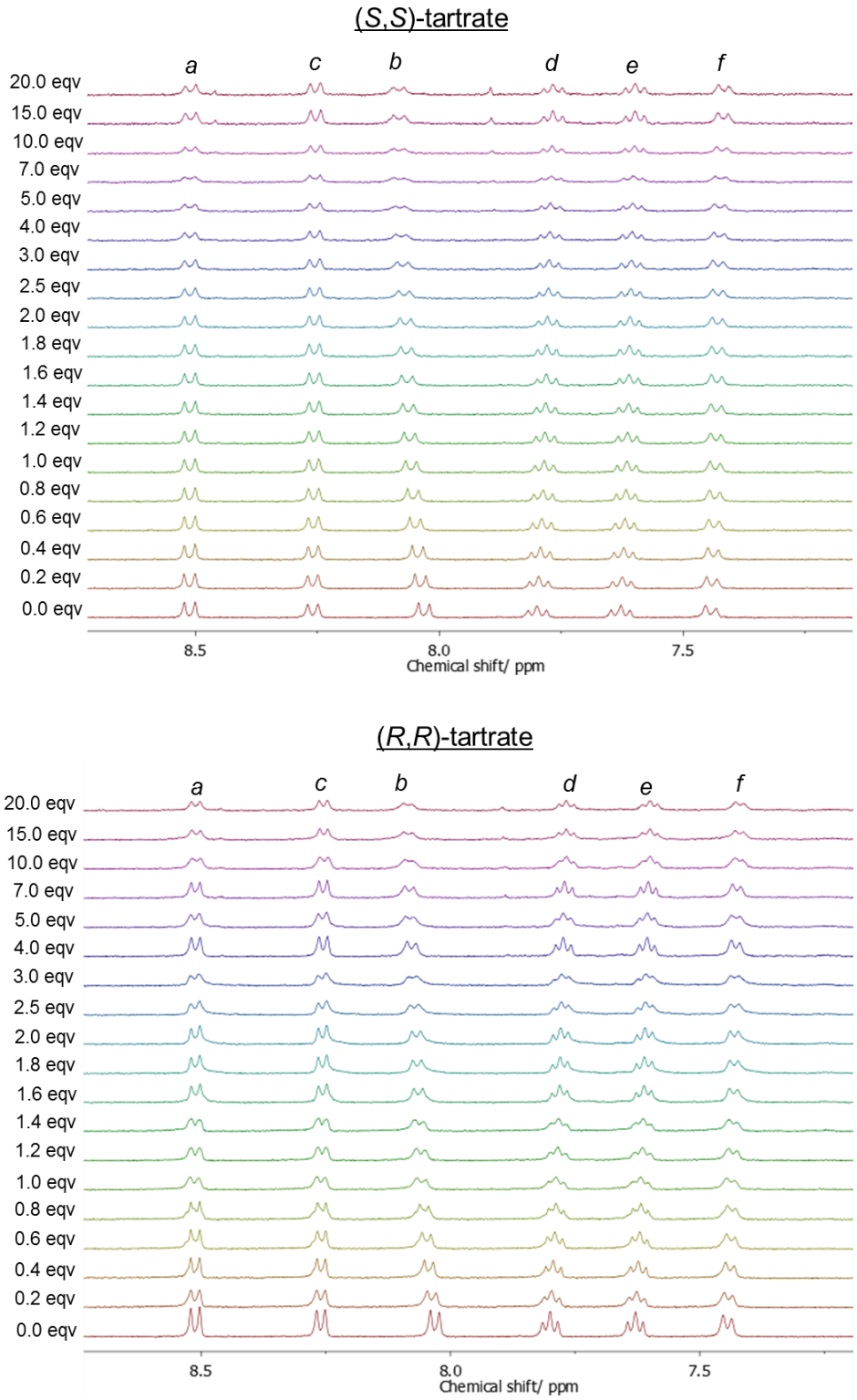

Fig. S3-1. Stacked partial ^{1}H NMR spectra showing the aromatic region of **1.XB** with increasing equivalents of (*S*,*S*)-tartrate (top) and (*R*,*R*)-tartrate (bottom) ([**1.XB**] = 1.0 mM, d_6-acetone/ D_2O 85:15 *v/v*, *T* = 298 K). Proton assignments follow those in Fig S2-1.

NBoc-Glutamate Enantiomers

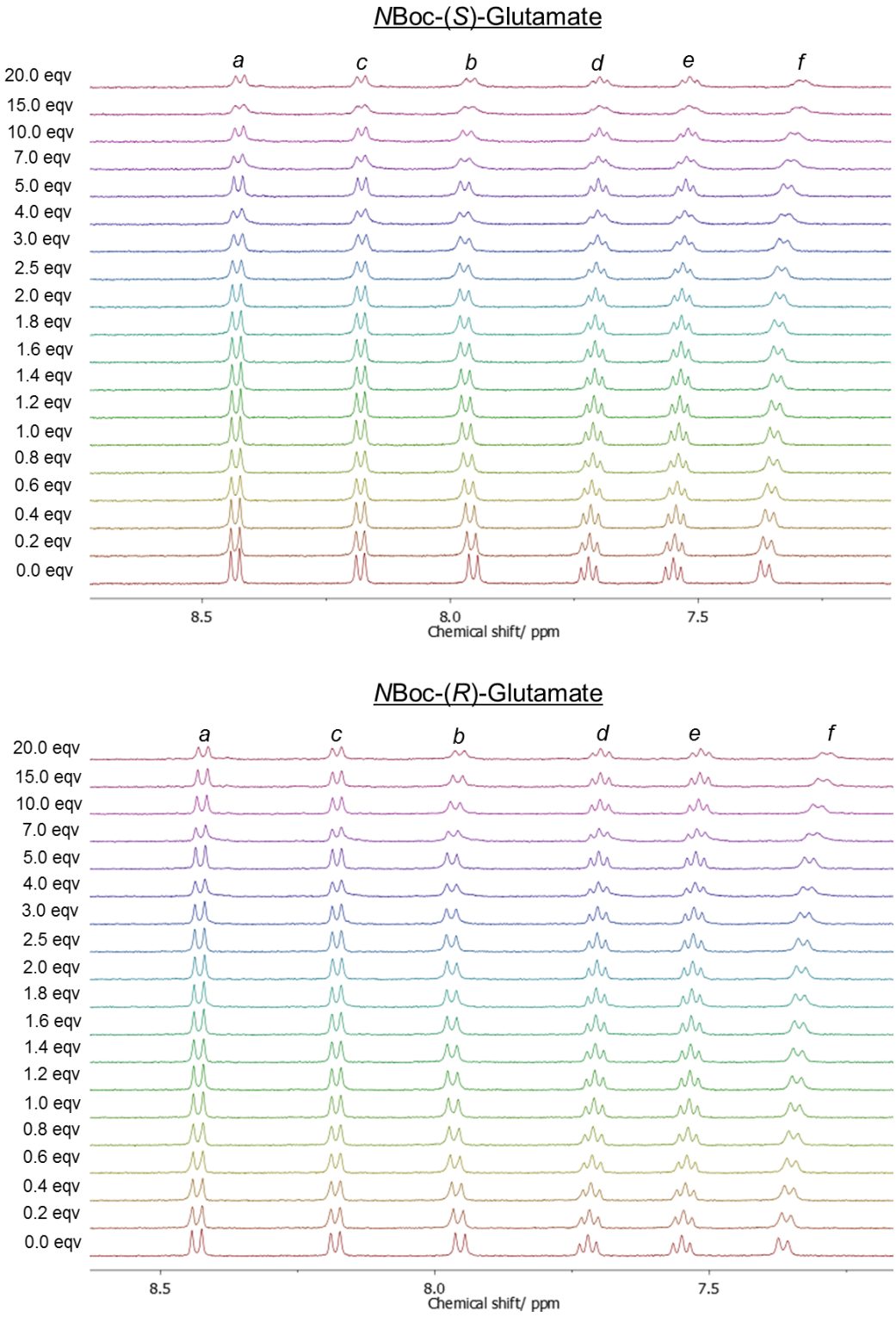

Fig. S3-2. Stacked partial ^{1}H NMR spectra showing the aromatic region of **1.XB** with increasing equivalents of *N*Boc-(*S*)-glutamate (top) and *N*Boc-(*R*)-glutamate (bottom) ([**1.XB**] = 1.0 mM, d_6-acetone/ D_2O 85:15 *v/v*, *T* = 298 K). Proton assignments follow those in Fig S2-1.

Maleate/ Fumarate

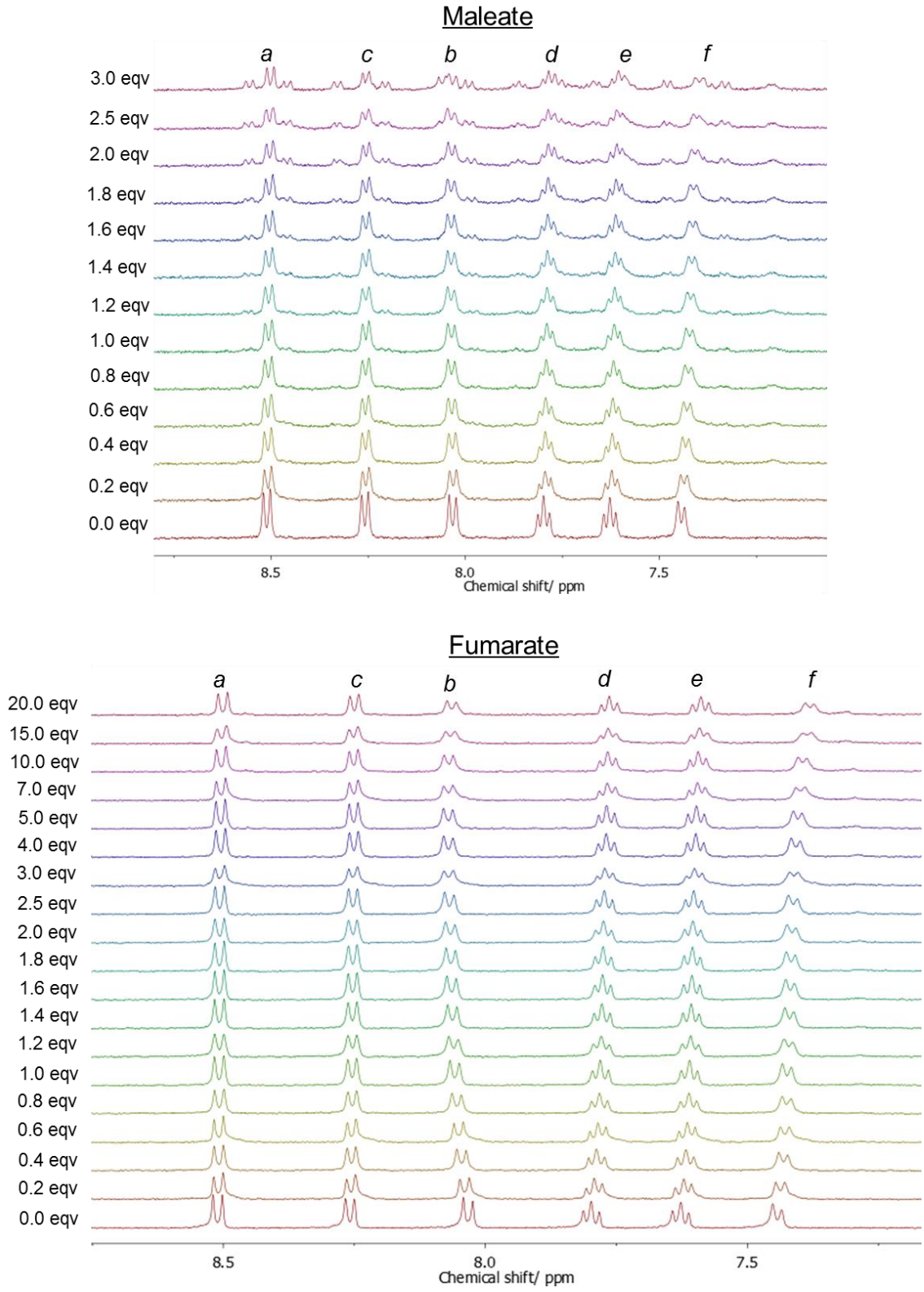

Fig. S3-3. Stacked partial ^{1}H NMR spectra showing the aromatic region of **1.XB** with increasing equivalents of maleate (top) and fumarate (bottom) ([**1.XB**] = 1.0 mM, d_6-acetone/ D_2O 85:15 *v/v*, *T* = 298 K). Proton assignments follow those in Fig S2-1.

Note: Due to obvious decomposition of **1.XB** seen during the maleate titration (top), no further anion was added after 3.0 equivalents, and no reliable association constants could be obtained.

Phthalate/ Isopthalate

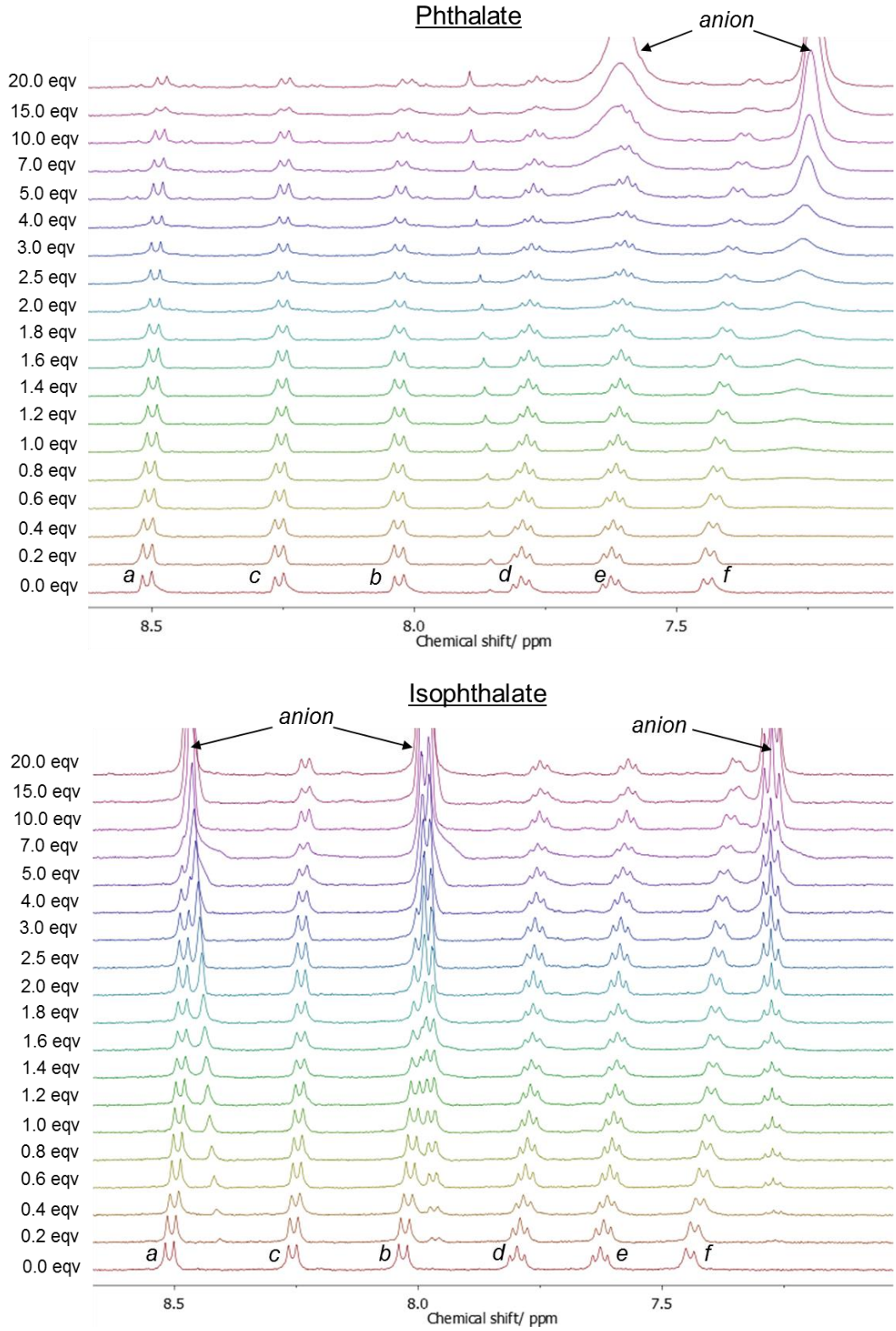

Fig. S3-4. Stacked partial ^{1}H NMR spectra showing the aromatic region of **1.XB** with increasing equivalents of phthalate (top) and isophthalate (bottom) ([**1.XB**] = 1.0 mM, d_6-acetone/ D_2O 85:15 *v/v*, *T* = 298 K). Proton assignments follow those in Fig S2-1.

Anion Binding Isotherms for 1.XB

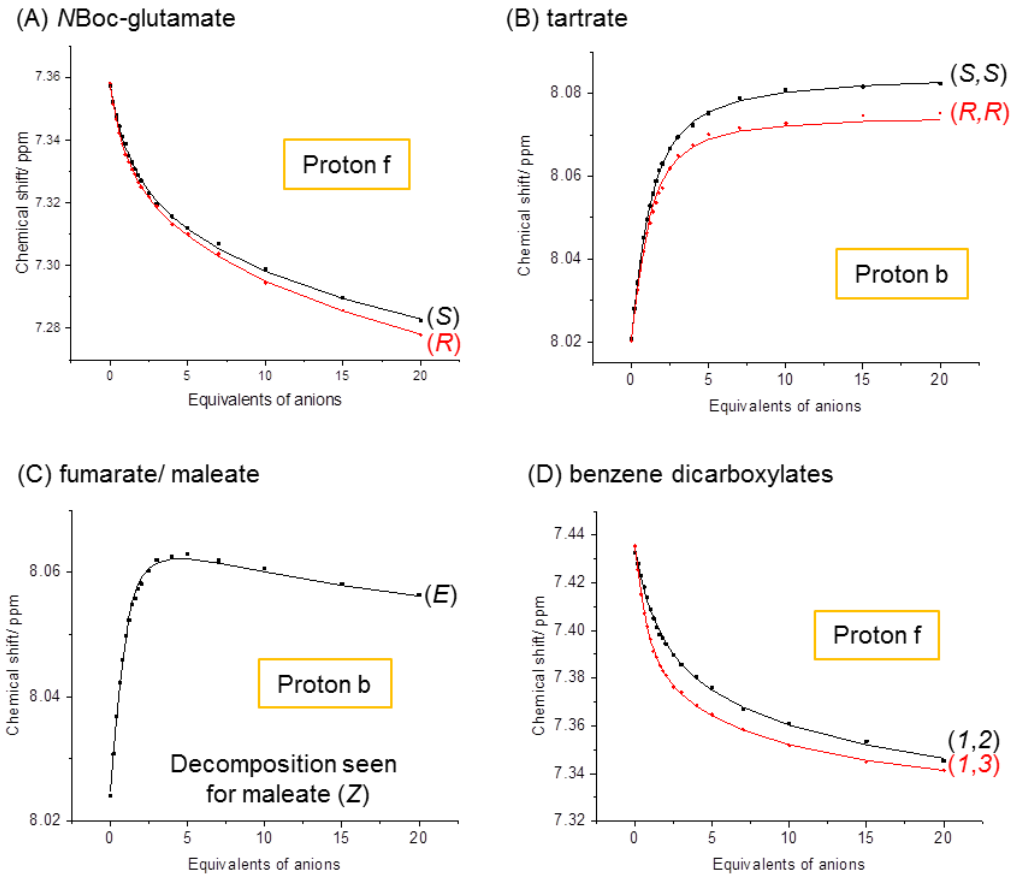

Fig. S3-5. Binding isotherms using a host-guest 1:2 model (K_2 < 10 M^{-1} in all cases) showing the changes in the chemical shift of either proton H_b or H_f (indicated) of receptor **1.XB** (assignment in Fig. S2-1) with increasing equivalents of (A) *N*Boc-(*S*/*R*)-glutamate; (B) (*S*,*S*) or (*R*,*R*)-tartrate; (C) fumarate/ maleate; (D) benzene dicarboxylates ([**1.XB**] = 1.0 mM, d_6-acetone/ D_2O 85:15 *v/v*, *T* = 298 K).

Receptor 1.HB

Due to the acidity of the triazolium aromatic protons, deuterium exchange was observed with the D_2O present, and hence they could not be monitored throughout the titrations.

Tartrate Enantiomers

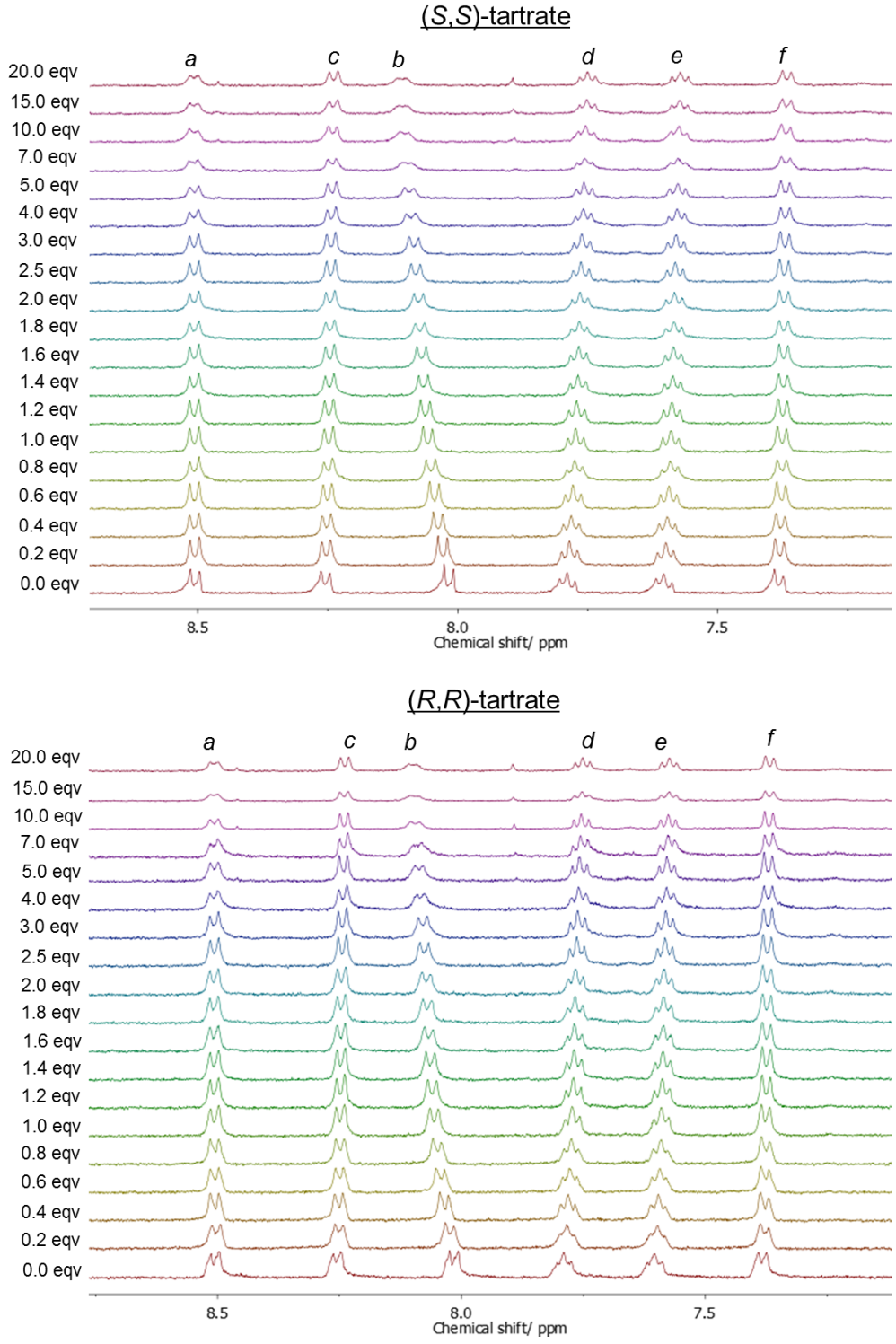

Fig. S3-6. Stacked partial ^{1}H NMR spectra showing the aromatic region of **1.HB** with increasing equivalents of (*S*,*S*)-tartrate (top) and (*R*,*R*)-tartrate (bottom) ([**1.HB**] = 1.0 mM, d_6-acetone/ D_2O 85:15 *v/v*, *T* = 298 K). Proton assignments follow those in Fig S2-4.

NBoc-Glutamate Enantiomers

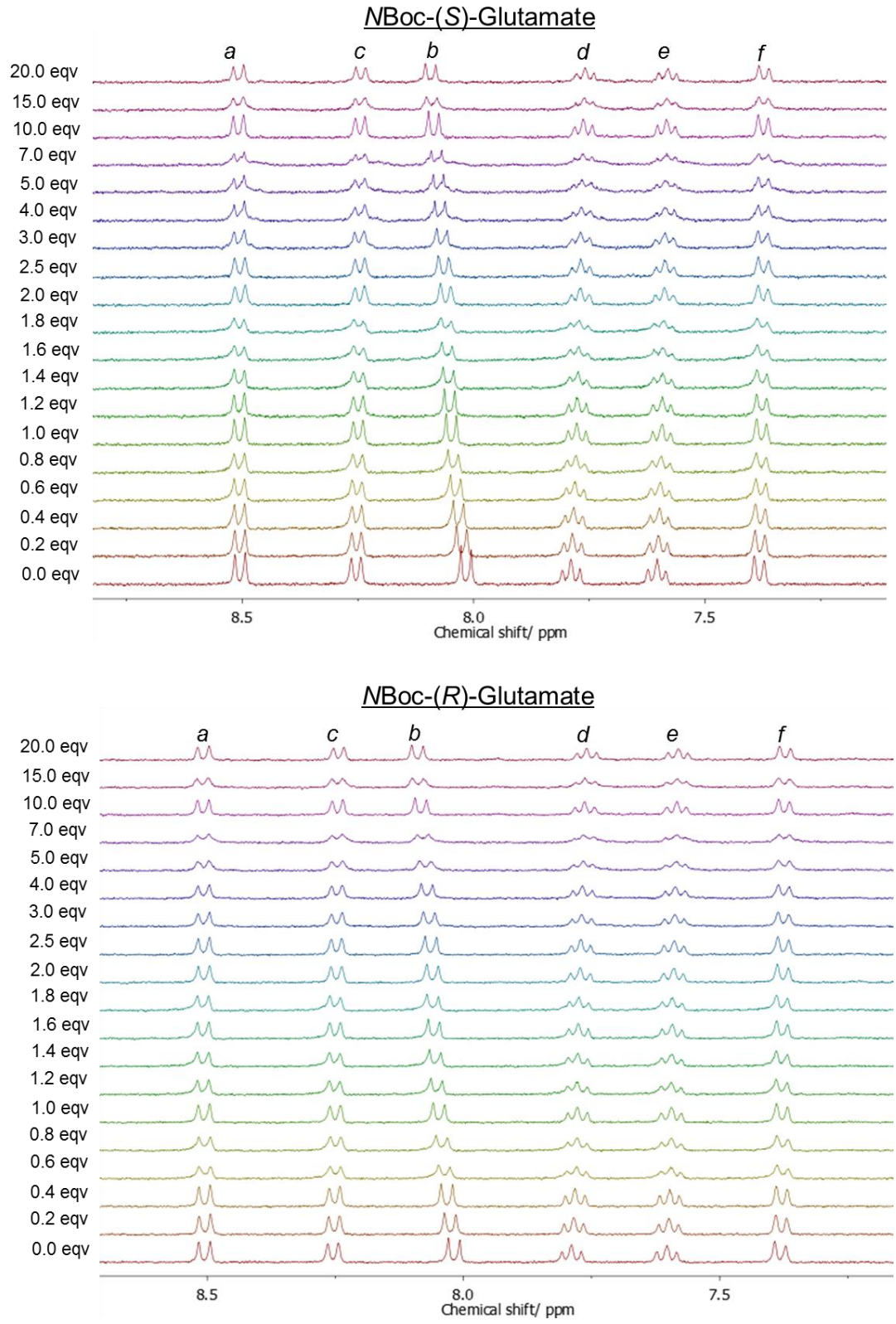

Fig. S3-7. Stacked partial ^{1}H NMR spectra showing the aromatic region of **1.HB** with increasing equivalents of *N*Boc-(*S*)-glutamate (top) and *N*Boc-(*R*)-glutamate (bottom) ([**1.HB**] = 1.0 mM, d_6-acetone/ D_2O 85:15 *v/v*, *T* = 298 K). Proton assignments follow those in Fig S2-4.

Maleate/ Fumarate

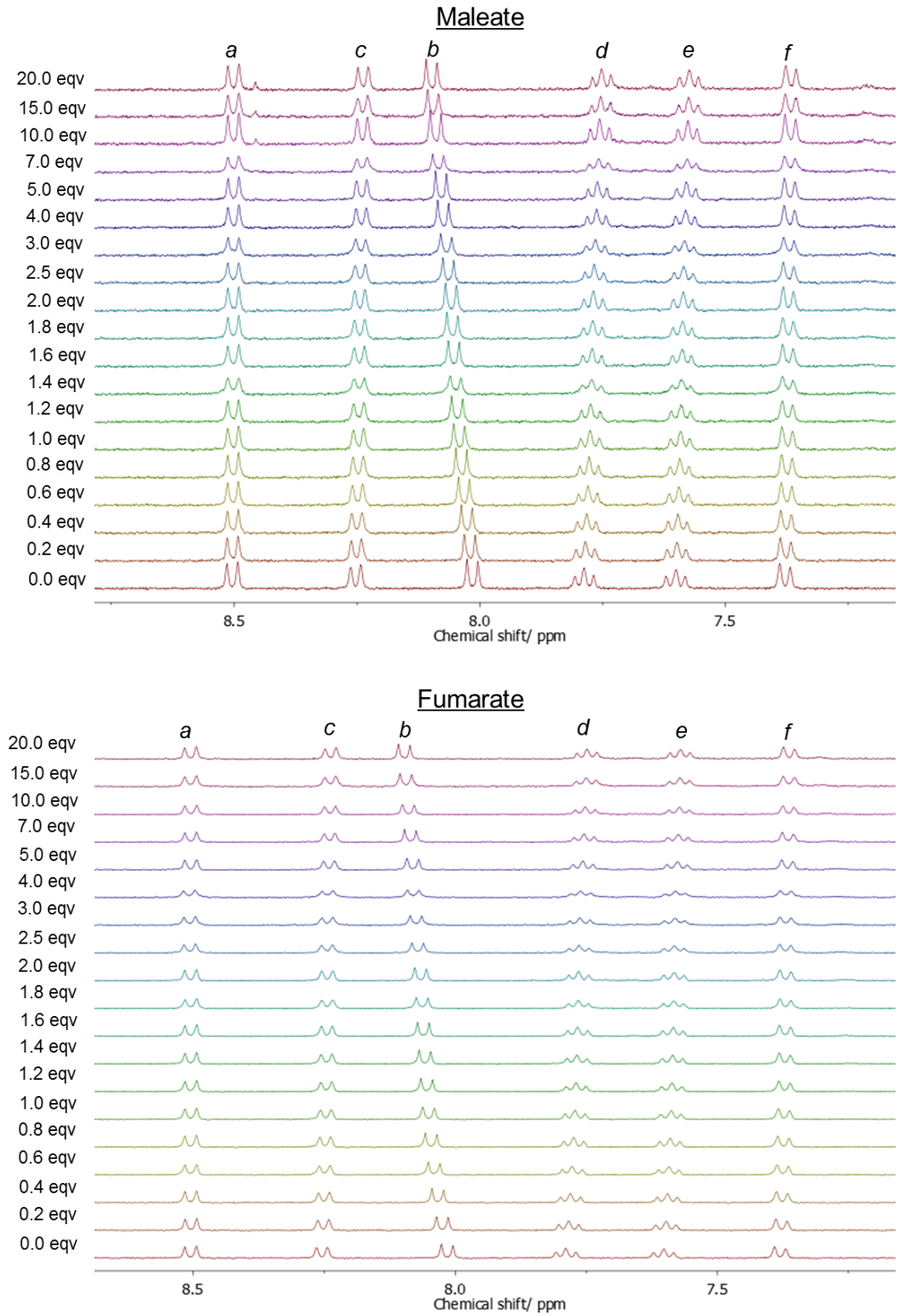

Fig. S3-8. Stacked partial ^{1}H NMR spectra showing the aromatic region of **1.HB** with increasing equivalents of maleate (top) and fumarate (bottom) ([**1.HB**] = 1.0 mM, d_6-acetone/ D_2O 85:15 *v/v*, *T* = 298 K). Proton assignments follow those in Fig S2-4.

Phthalate/ Isopthalate

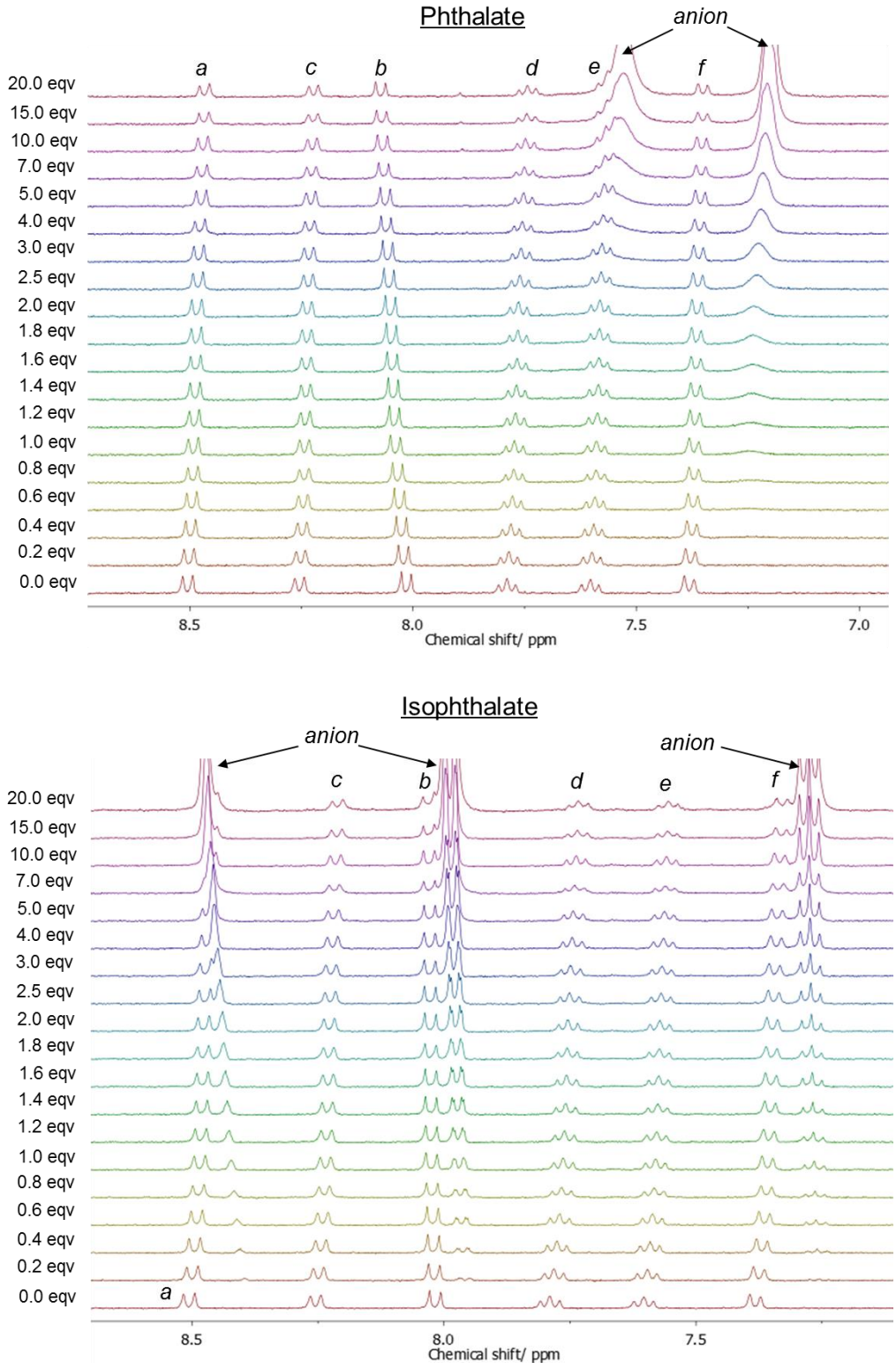

Fig. S3-9. Stacked partial ^{1}H NMR spectra showing the aromatic region of **1.HB** with increasing equivalents of phthalate (top) and isophthalate (bottom) ([**1.HB**] = 1.0 mM, d_6-acetone/ D_2O 85:15 *v/v*, *T* = 298 K). Proton assignments follow those in Fig S2-4.

Anion Binding Isotherms for 1.HB

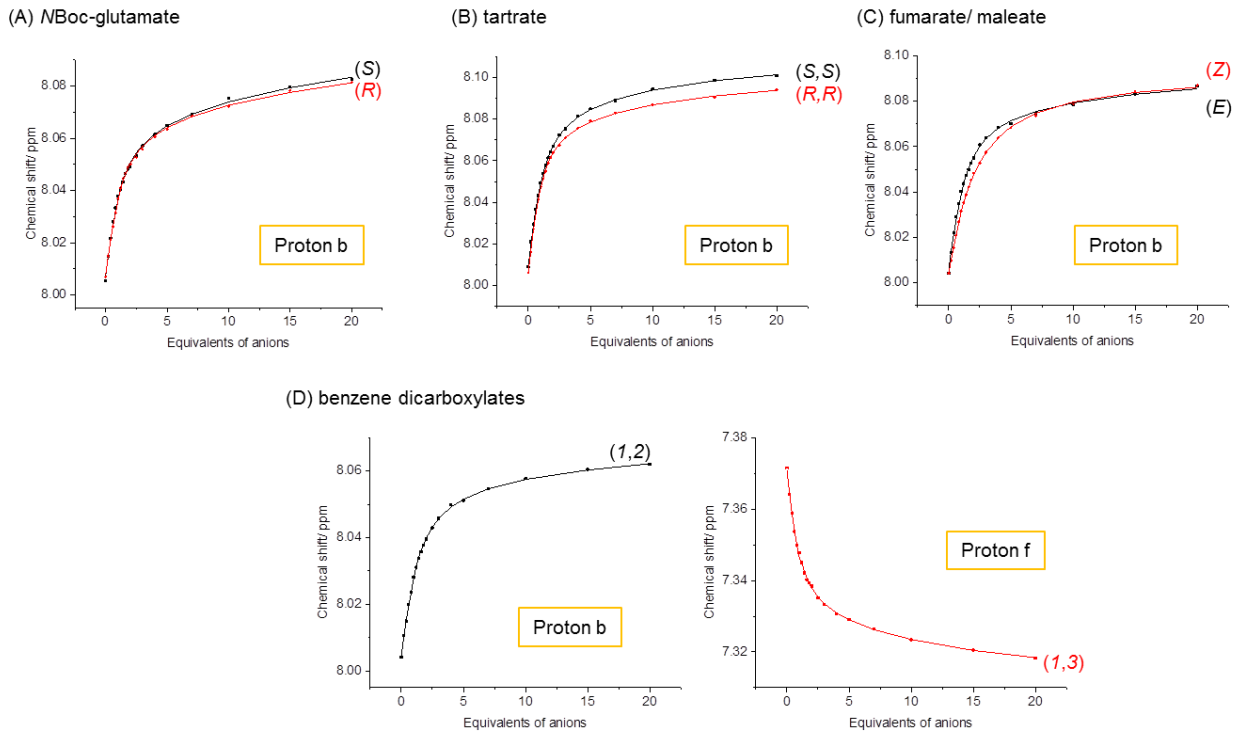

Fig. S3-10. Binding isotherms using a host-guest 1:2 model (K_2 < 10 M^{-1} in all cases) showing the changes in the chemical shift of either proton H_b or H_f (indicated) of receptor **1.HB** (assignment in Fig. S2-4) with increasing equivalents of (A) *N*Boc-(*S*/*R*)-glutamate; (B) (*S*,*S*) or (*R*,*R*)-tartrate; (C) fumarate/ maleate; (D) benzene dicarboxylates ([**1.HB**] = 1.0 mM, d_6-acetone/ D_2O 85:15 *v/v*, *T* = 298 K).

Receptor 1.ChB

Tartrate Enantiomers

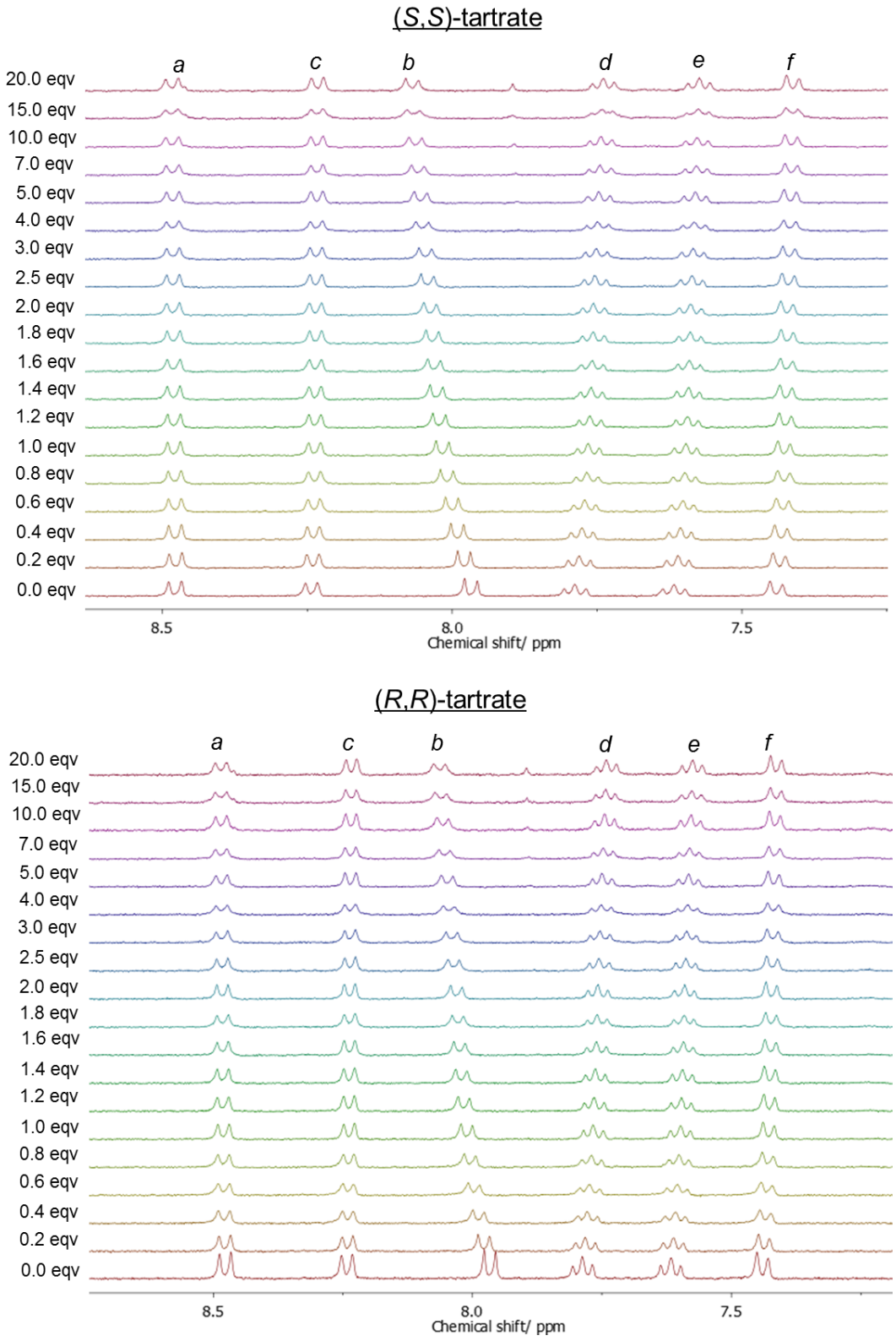

Fig. S3-11. Stacked partial ^{1}H NMR spectra showing the aromatic region of **1.ChB** with increasing equivalents of (*S*,*S*)-tartrate (top) and (*R*,*R*)-tartrate (bottom) ([**1.ChB**] = 1.0 mM, d_6-acetone/ D_2O 85:15 *v/v*, *T* = 298 K). Proton assignments follow those in Fig S2-7.

NBoc-Glutamate Enantiomers

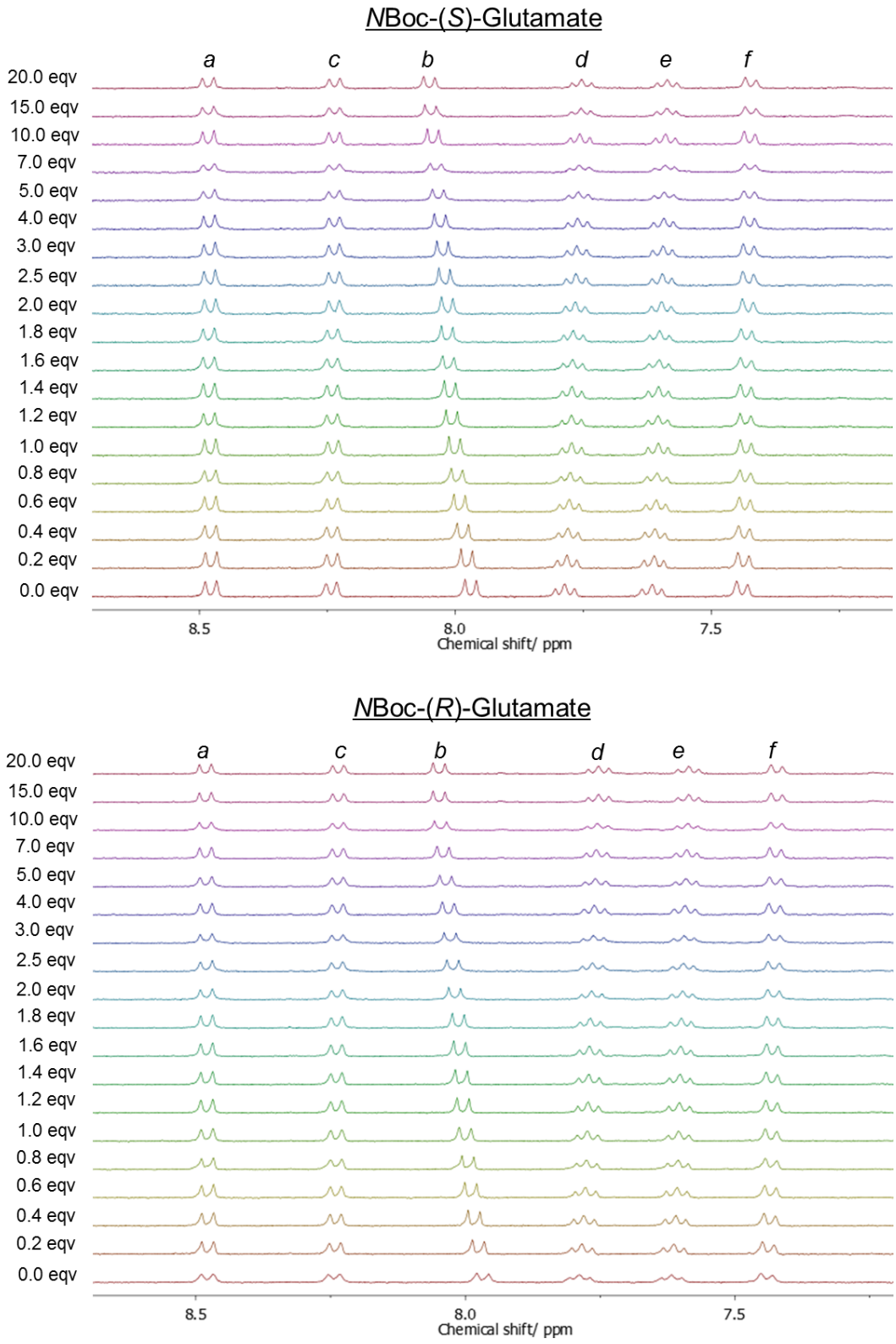

Fig. S3-12. Stacked partial ^{1}H NMR spectra showing the aromatic region of **1.ChB** with increasing equivalents of *N*Boc-(*S*)-glutamate (top) and *N*Boc-(*R*)-glutamate (bottom) ([**1.ChB**] = 1.0 mM, d_6-acetone/ D_2O 85:15 *v/v*, *T* = 298 K). Proton assignments follow those in Fig S2-7.

Maleate/ Fumarate

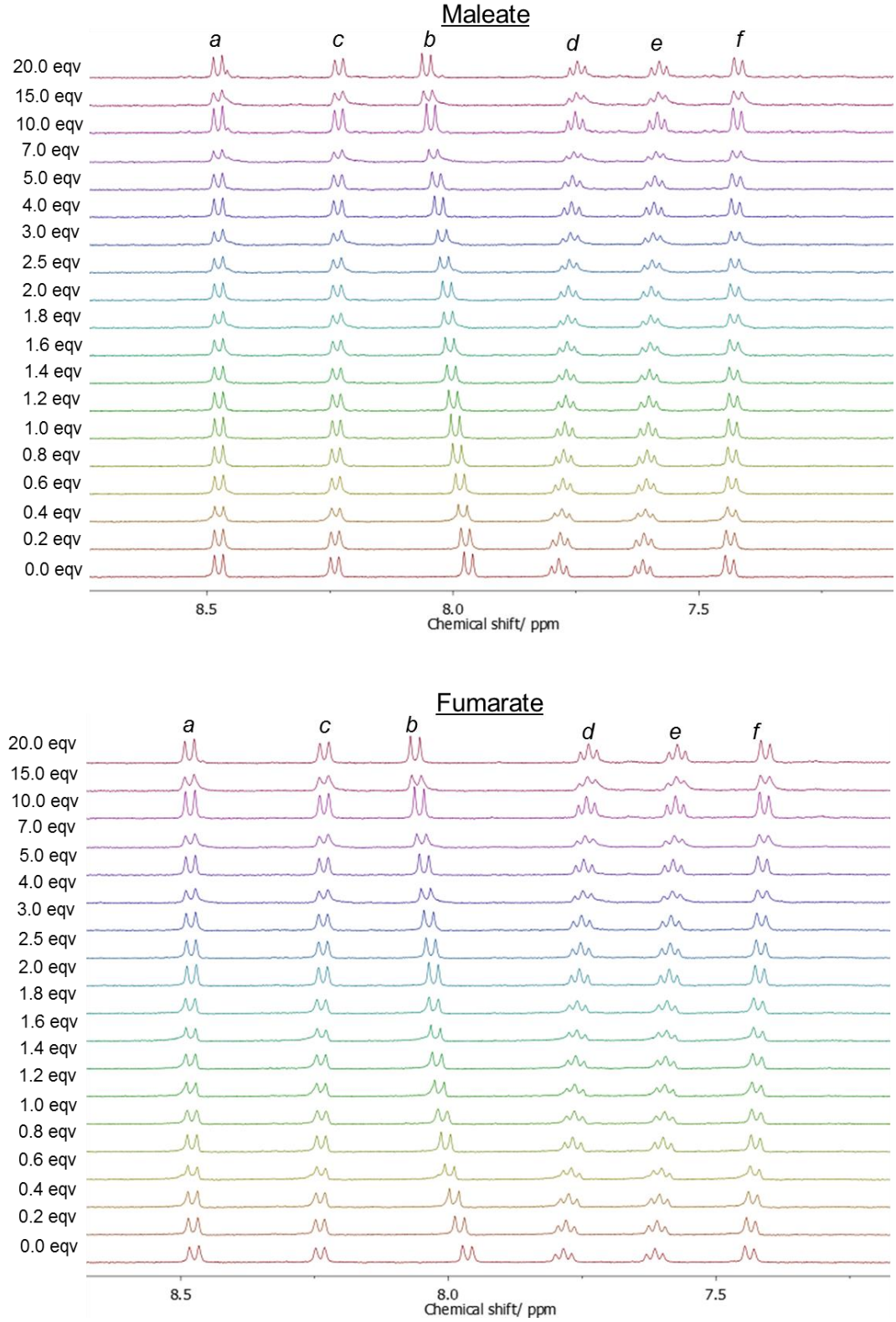

Fig. S3-13. Stacked partial ^{1}H NMR spectra showing the aromatic region of **1.ChB** with increasing equivalents of maleate (top) and fumarate (bottom) ([**1.ChB**] = 1.0 mM, d_6-acetone/ D_2O 85:15 *v/v*, *T* = 298 K). Proton assignments follow those in Fig S2-7.

Phthalate/ Isopthalate

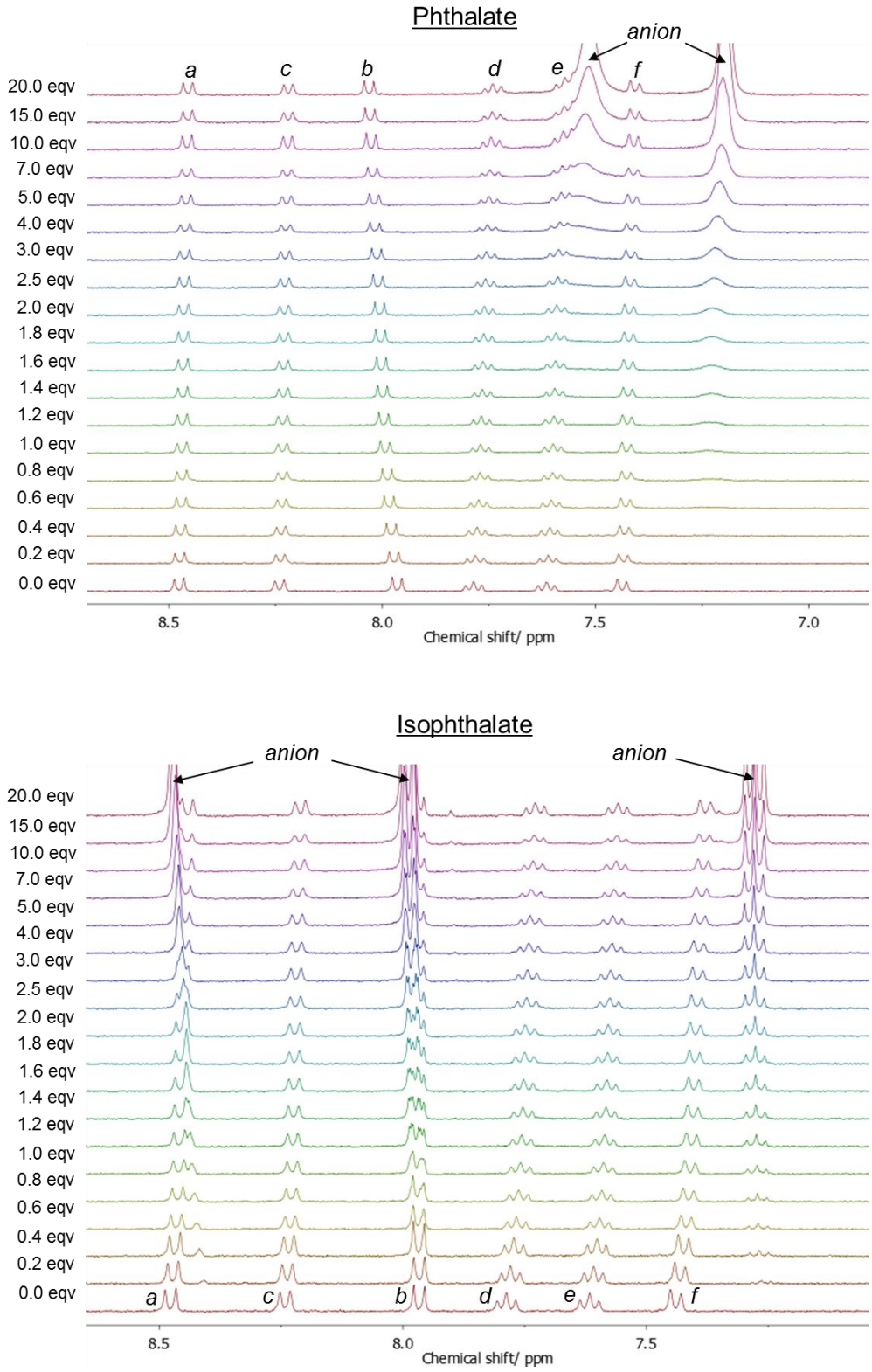

Fig. S3-14. Stacked partial ^{1}H NMR spectra showing the aromatic region of **1.ChB** with increasing equivalents of phthalate (top) and isophthalate (bottom) ([**1.ChB**] = 1.0 mM, d_6-acetone/ D_2O 85:15 *v/v*, *T* = 298 K). Proton assignments follow those in Fig S2-7.

Anion Binding Isotherms for 1.ChB

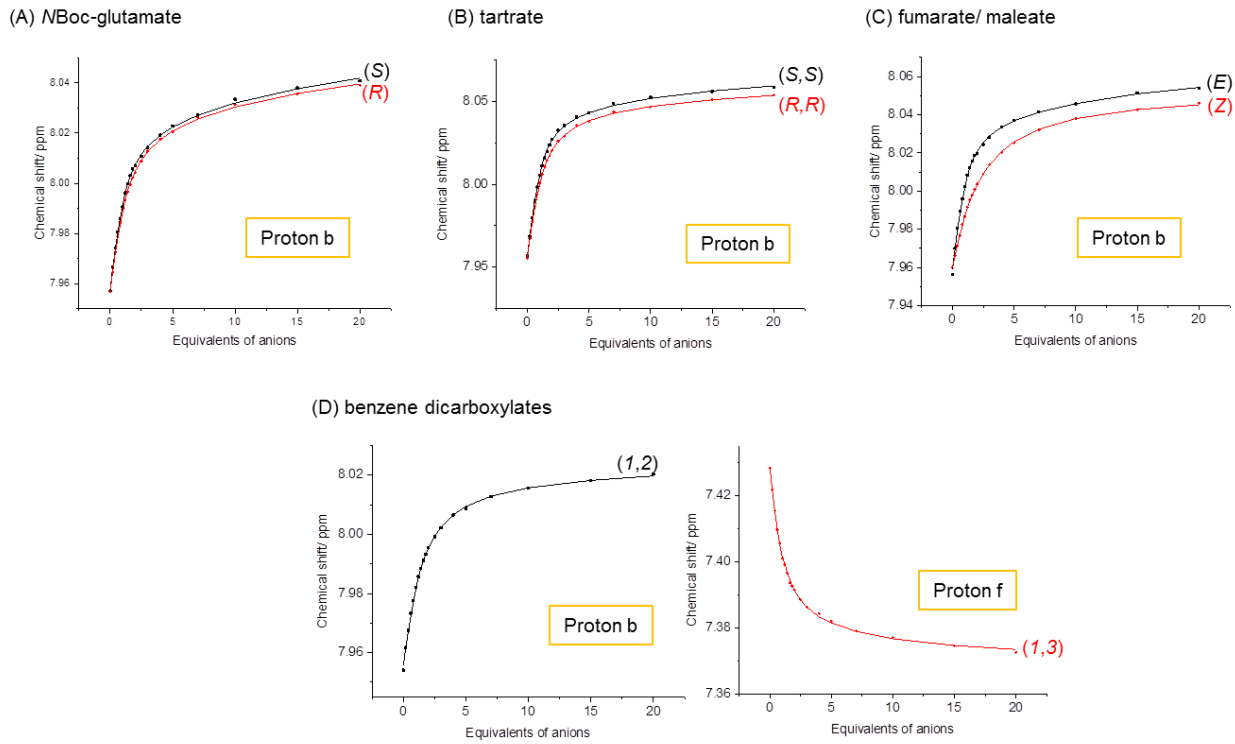

Fig. S3-15. Binding isotherms using a host-guest 1:2 model (K_2 < 10 M^{-1} in all cases) showing the changes in the chemical shift of either proton H_b or H_f (indicated) of receptor **1.ChB** (assignment in Fig. S2-7) with increasing equivalents of (A) NBoc-(*S*/*R*)-glutamate; (B) (*S*,*S*) or (*R*,*R*)-tartrate; (C) fumarate/ maleate; (D) benzene dicarboxylates ([**1.ChB**] = 1.0 mM, d_6-acetone/ D_2O 85:15 *v*/*v*, *T* = 298 K).

Table S3-1. Anion association constants (K/ M^{-1}) of receptors **1.XB**, **1.ChB** and **1.HB** with various anion stereo- and geometric isomers.[a]

Anion	1.XB	1.ChB	1.HB
*N*Boc-(*S*)-glutamate [b]	K_{11} = 1642 (63) K_{12} = 21 (1) [c]	K_{11} = 1949 (66) K_{12} = 28 (1)	K_{11} = 1863 (99) K_{12} = 24 (2)
*N*Boc-(*R*)-glutamate [b]	K_{11} = 2353 (53) K_{12} = 29 (1) [c]	K_{11} = 1717 (50) K_{12} = 31 (1)	K_{11} = 1949 (67) K_{12} = 22 (1)
(*S*,*S*)-tartrate	K_{11} = 3565 (89) K_{12} = 223 (6)	K_{11} = 2631 (66) K_{12} = 70 (5)	K_{11} = 2348 (96) K_{12} = 55 (4)
(*R*,*R*)-tartrate	K_{11} = 1815 (92) K_{12} = 81 (5)	K_{11} = 2411 (55) K_{12} = 65 (4)	K_{11} = 3412 (147) K_{12} = 59 (3)
Maleate	- [d]	K_{11} = 532 (10) [e]	K_{11} = 596 (13) [e]
Fumarate	K_{11} = 3183 (53) K_{12} = 32 (1)	K_{11} = 2926 (93) K_{12} = 39 (1)	K_{11} = 1216 (78) [e]
Phthalate	K_{11} = 1336 (139) K_{12} = 49 (6) [c,f]	K_{11} = 1858 (48) K_{12} = 80 (4)	K_{11} = 1343 (32) K_{12} = 15(2)
Isophthalate	K_{11} = 7774 (769) K_{12} = 93 (4) [c]	K_{11} = 6502 (640) K_{12} = 78 (8) [c]	K_{11} = 4161 (395) K_{12} = 50 (5) [c]

[a] Proton H_b monitored and data fit to a host-guest 1:2 stoichiometric binding model with BindFit[3] unless otherwise stated; errors (±) in parentheses; [host] = 1.0 mM, d_6-acetone/ D_2O 85:15 *v/v*, T = 298 K. [b] As no reasonable data fit could be obtained with the BindFit software, WinEQNMR2[4] was used to fit the titration data for *N*Boc-glutamate; [c] H_f monitored due to small perturbations of H_b which prevented data from being fitted accurately; [d] receptor decomposition observed on anion addition; [e] No evidence of second binding event occurring, hence data fit only to a host-guest 1:1 model; [f] slight receptor decomposition seen at 10 eqv. of phthalate, hence values reported are only estimates.

Table S3-2. Selectivities (ξ) of receptors **1.XB**, **1.ChB** and **1.HB** for dicarboxylate enantiomers and geometric isomers.[a]

Anions	ξ	1.XB	1.ChB	1.HB
Tartrate	$K_{S,S}$/ $K_{R,R}$	2.0 (0.1)	1.09 (0.04)	0.69 (0.04)
*N*Boc-glut	K_S/ K_R	0.70 (0.03)	1.14 (0.05)	0.96 (0.06)
Fumarate/ maleate	K_{fum}/ K_{mal}	-[b]	5.5 (0.2)	2.0 (0.1)
Benzene dicarboxylates	K_{iso}/ K_{phth}	5.8 (0.8)	3.5 (0.4)	3.1 (0.3)

[a] ξ calculated from K_{11} values, errors (±) in parentheses; ([host] = 1.0 mM, d_6-acetone/ D_2O 85:15 *v/v*, T = 298 K. [b] not determined due to **1.XB** decomposition by maleate.

S4. Fluorescence Anion Sensing

General procedure

Fluorescence titration experiments were performed using a Horiba Fluorolog 3 at 293 K. The host molecules (**1.XB/ ChB/ HB**) were dissolved in acetone/H_2O 85:15 *v/v* to give a concentration of 50 μM. The TBA salt of the dicarboxylate was dissolved in the solution of the host molecule to obtain a concentration of 75 mM. Aliquots of the anion solution were added to 0.75 mL of the host solution in a quartz cuvette, where the sample was then thoroughly mixed before fluorescence spectra were recorded.

Fluorescence spectra

Receptor 1.XB

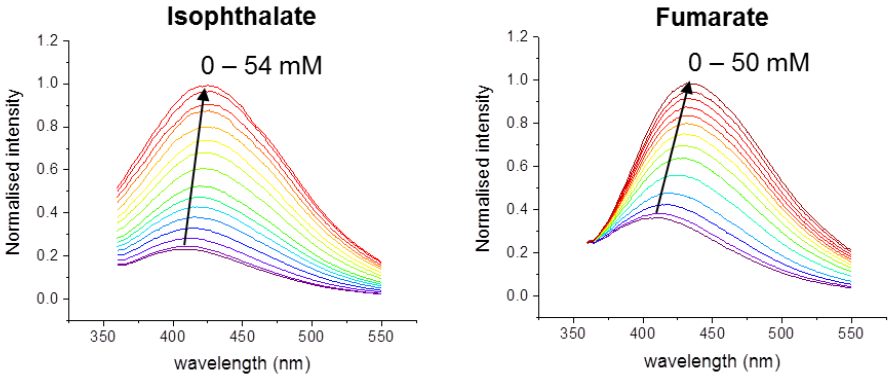

Fig. S4-1. Fluorescence spectra of receptor **1.XB** in the presence of increasing quantities of dicarboxylate geometric isomers ([**1.XB**] = 50 μM; λ_{ex} = 325 nm; slit width 4 nm; acetone/ water 85:15 *v/v*, *T* = 298 K). Spectra for phthalate and maleate not shown due to receptor decomposition during the titrations. Concentrations of anions added are indicated, together with the direction of intensity change.

Receptor 1.HB

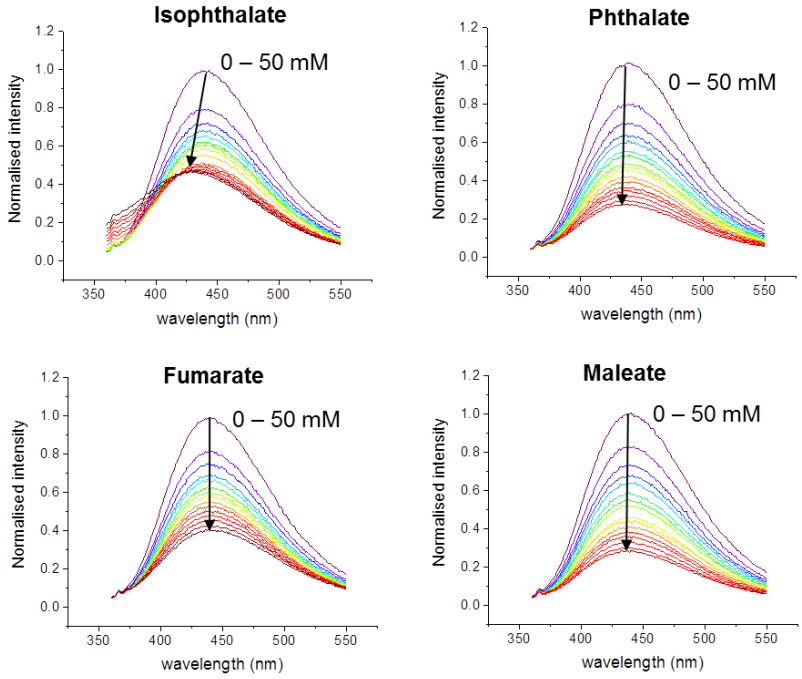

Fig. S4-2. Fluorescence spectra of receptor **1.HB** in the presence of increasing quantities of dicarboxylate geometric isomers ([**1.HB**] = 50 μM; λ_{ex} = 330 nm; slit width 1 nm; acetone/ water 85:15 *v/v*, *T* = 298 K).

Receptor 1.ChB

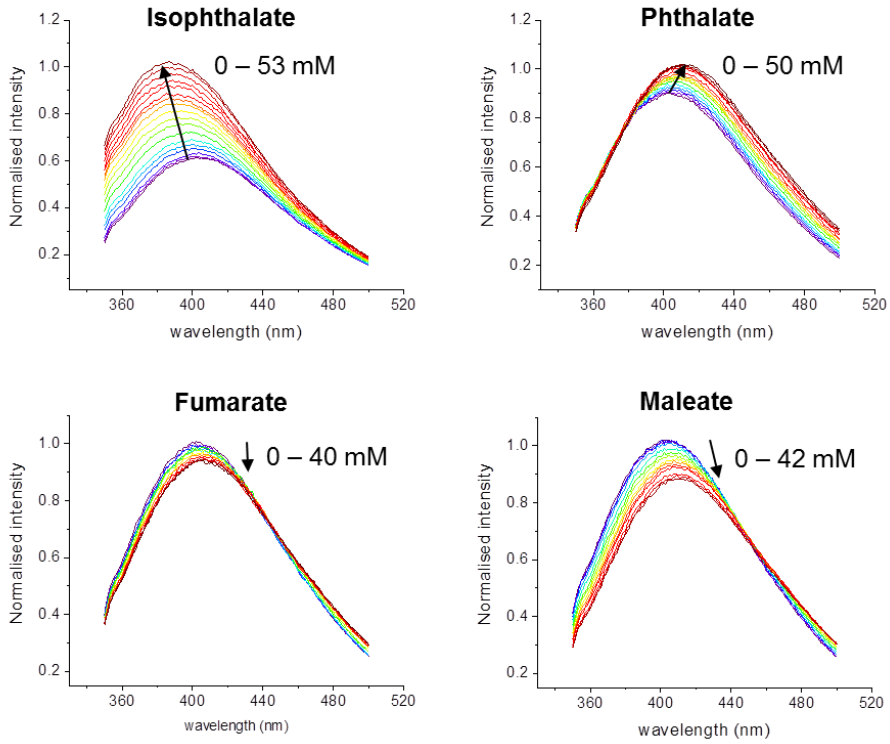

Fig. S4-3. Fluorescence spectra of receptor **1.ChB** in the presence of increasing quantities of dicarboxylate geometric isomers ([**1.ChB**] = 50 μM; λ_{ex} = 320 nm; slit width 3 nm; acetone/ water 85:15 *v/v*, *T* = 298 K).

S5. Molecular Modeling: Additional Data & Methods

S5.1. Additional Figures

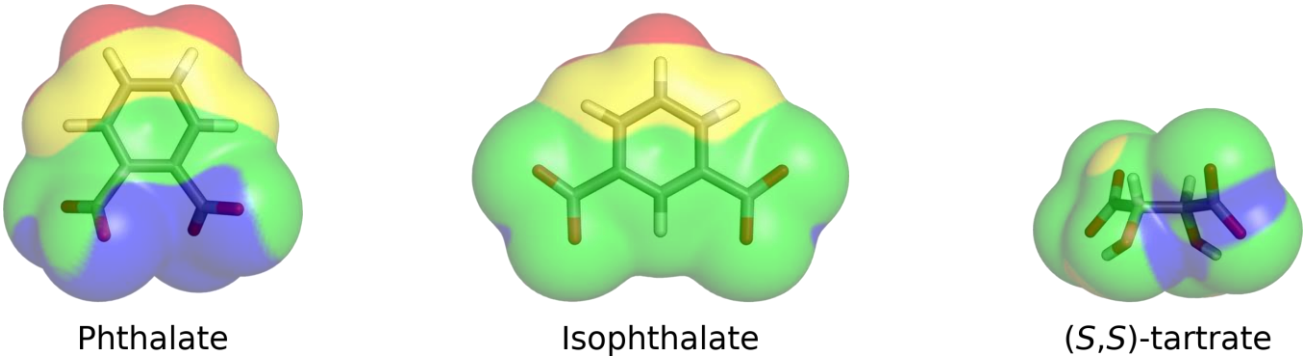

Fig. S5-1. Distribution of the electrostatic potential mapped on the 0.001 electrons Bohr^{-3} isodensity surface of phthalate, isophthalate and (S,S)-tartrate. The colour scale, in kcal mol^{-1}, is as follows: blue – lower than –193; green − from –193 to –160; yellow – from –160 to –127; and red − greater than –127.

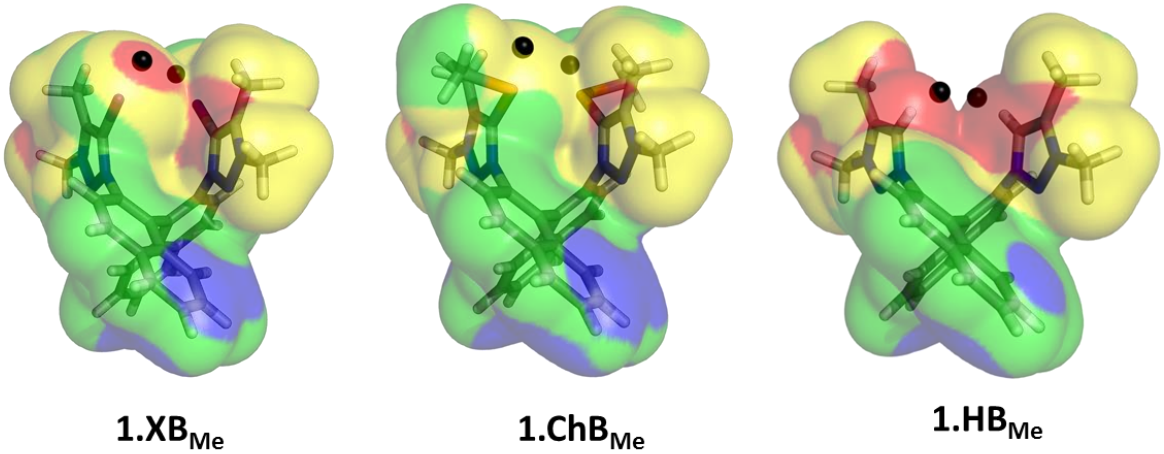

Fig. S5-2. Distribution of the electrostatic potential mapped on the 0.001 electrons Bohr^{-3} isodensity surface of **1.XB$_{Me}$**, **1.ChB$_{Me}$** and **1.HB$_{Me}$**. The colour scale, in kcal mol^{-1}, is as follows: blue – lower than 100; green − from 100 to 120; yellow − from 120 to 140; and red − greater than 140. The maxima in front of the binding units are identified with black dots.

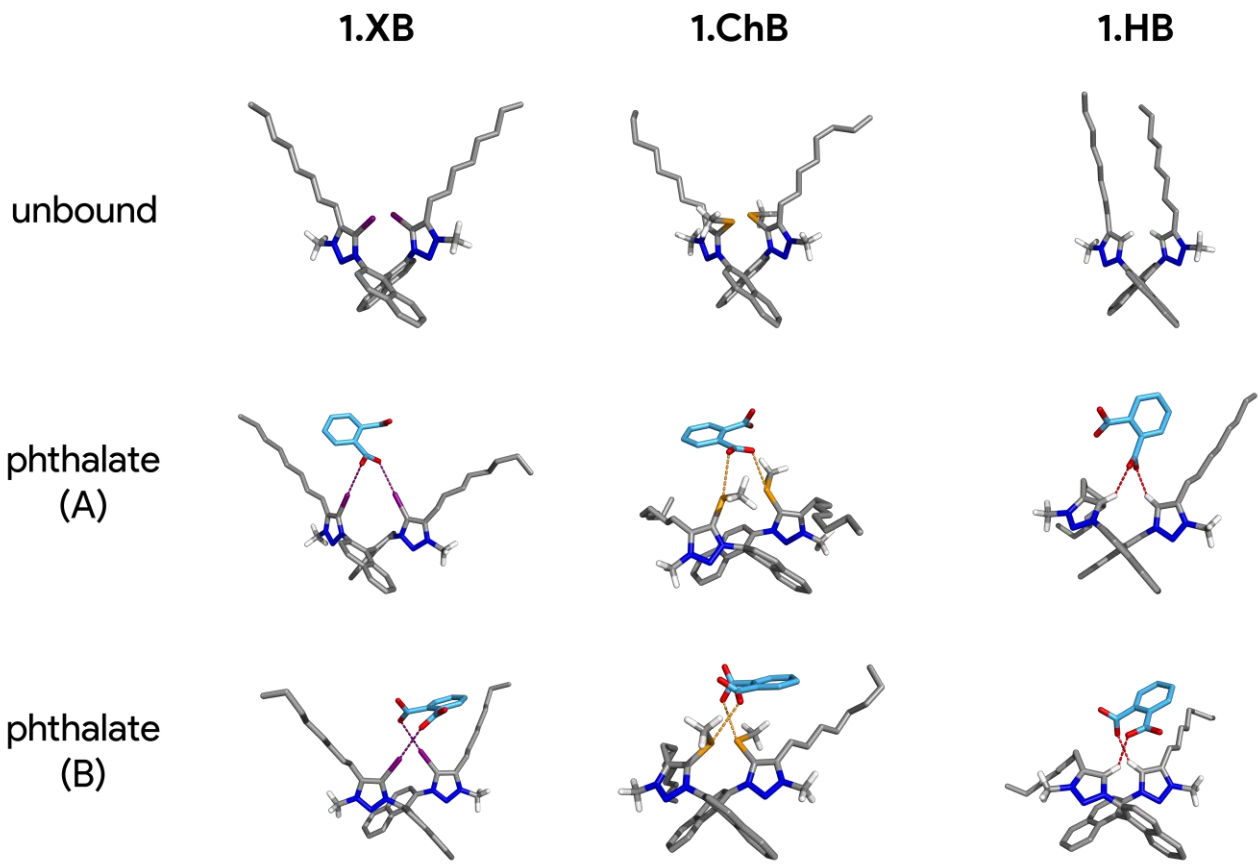

Fig. S5-3. Illustrative MD snapshots of the unbound receptor and phthalate complexed **1.XB**, **1.ChB** and **1.HB** in scenarios A and B. The XB, ChB and HB interactions are depicted as purple, orange and red dashed lines, respectively. Solvent molecules, PF_6^- counter-ions and most hydrogen atoms were hidden for clarity.

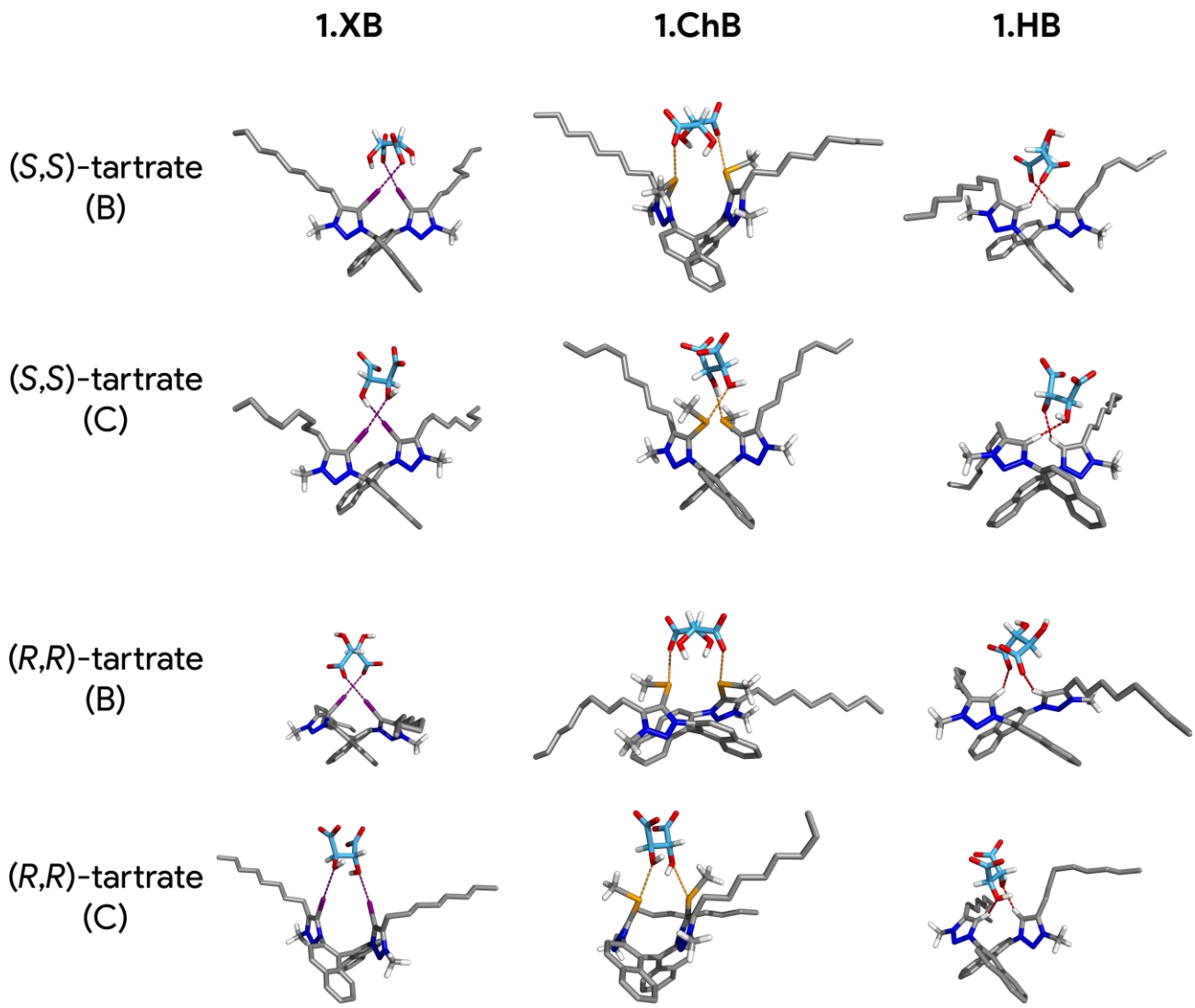

Fig. S5-4. Illustrative MD snapshots of the (*S*,*S*)- or (*R*,*R*)-tartrate complexes **1.XB**, **1.ChB** and **1.HB** in scenarios B and C. The XB, ChB and HB interactions are depicted as purple, orange and red dashed lines, respectively. Solvent molecules and most hydrogen atoms were hidden for clarity.

S5.2. Additional Tables

Table S5-1. Binding units V_S maxima, $z\cdots z$ distances[a] and α angles calculated from the DFT optimised structures of model receptors **1.XB$_{Me}$**, **1.ChB$_{Me}$** and **1.HB$_{Me}$**.

Receptor	Binding units V_S maxima (kcal mol^{-1})	$z\cdots z$ distances (Å)	α angles (°)
1.XB$_{Me}$	151.88 ; 151.83	4.226	91.5
1.ChB$_{Me}$	139.15 ; 139.13	3.807	89.4
1.HB$_{Me}$	162.25 ; 162.23	3.607	90.3

[a] z = I, Se or H for **1.XB$_{Me}$**, **1.ChB$_{Me}$** or **1.HB$_{Me}$**, respectively.

Table S5-2. Average intramolecular *z*···*z* distances[a,b] and α angles[b], along with corresponding standard deviations (SD), estimated from the concatenated molecular dynamics simulations of unbound and bound **1.XB**, **1.ChB** and **1.HB**.

Receptor	Anion	Scenario	*z*···*z* distances (Å)		α angles (°)	
			Avg ± SD	Range	Avg ± SD	Range
1.XB	Unbound	--	3.991 ± 0.121	[3.587 ; 4.734]	94.7 ± 8.5	[58.4 ; 125.9]
	Phthalate	A	3.637 ± 0.107	[3.266 ; 4.145]	97.0 ± 7.5	[65.6 ; 125.5]
		B	3.591 ± 0.106	[3.254 ; 4.110]	96.4 ± 7.6	[64.7 ; 126.1]
	Isophthalate	A	3.664 ± 0.112	[3.296 ; 4.174]	96.7 ± 7.5	[67.8 ; 128.3]
		B	3.788 ± 0.131	[3.377 ; 4.551]	91.9 ± 8.0	[56.3 ; 124.1]
	(*S*,*S*)-tartrate	B	3.853 ± 0.156	[3.350 ; 4.608]	91.5 ± 7.7	[60.9 ; 122.2]
		C	3.671 ± 0.129	[3.264 ; 4.428]	95.8 ± 7.7	[65.3 ; 126.2]
	(*R*,*R*)-tartrate	B	3.683 ± 0.127	[3.276 ; 4.401]	100.8 ± 6.8	[71.2 ; 129.5]
		C	3.661 ± 0.126	[3.226 ; 4.292]	96.2 ± 7.6	[64.1 ; 125.7]
1.ChB	Unbound	--	3.815 ± 0.175	[3.360 ; 4.965]	98.1 ± 8.2	[63.8 ; 127.3]
	Phthalate	A	3.437 ± 0.131	[3.066 ; 4.329]	101.3 ± 7.5	[66.3 ; 132.4]
		B	3.395 ± 0.108	[3.020 ; 4.063]	97.2 ± 7.5	[65.6 ; 125.7]
	Isophthalate	A	3.407 ± 0.107	[3.076 ; 4.137]	99.6 ± 7.5	[67.4 ; 130.9]
		B	3.502 ± 0.115	[3.120 ; 4.219]	94.2 ± 8.0	[59.4 ; 125.3]
	(*S*,*S*)-tartrate	B	3.687 ± 0.146	[3.194 ; 4.476]	93.6 ± 7.7	[62.0 ; 124.7]
		C	3.553 ± 0.125	[3.142 ; 4.291]	96.2 ± 7.9	[60.3 ; 125.7]
	(*R*,*R*)-tartrate	B	3.703 ± 0.300	[3.124 ; 5.523]	100.6 ± 6.8	[68.1 ; 127.6]
		C	3.395 ± 0.108	[3.034 ; 4.099]	98.1 ± 7.6	[62.3 ; 131.6]
1.HB	Unbound	--	3.210 ± 0.427	[1.843 ; 5.270]	89.9 ± 9.3	[52.8 ; 124.7]
	Phthalate	A	2.491 ± 0.321	[1.781 ; 4.338]	96.5 ± 8.3	[61.2 ; 129.4]
		B	3.040 ± 0.592	[1.833 ; 5.396]	93.1 ± 8.4	[55.2 ; 124.4]
	Isophthalate	A	2.404 ± 0.307	[1.745 ; 4.300]	98.9 ± 8.4	[62.5 ; 129.1]
		B	3.520 ± 0.412	[2.206 ; 5.396]	90.4 ± 8.7	[53.4 ; 128.3]
	(*S*,*S*)-tartrate	B	2.999 ± 0.707	[1.794 ; 6.132]	93.7 ± 8.4	[53.1 ; 125.0]
		C	2.463 ± 0.286	[1.767 ; 4.606]	98.2 ± 8.2	[59.5 ; 130.4]
	(*R*,*R*)-tartrate	B	2.308 ± 0.196	[1.768 ; 3.273]	101.3 ± 7.0	[61.2 ; 128.3]
		C	2.493 ± 0.329	[1.776 ; 5.028]	98.0 ± 8.2	[64.4 ; 127.1]

[a] *z* = I, Se or H binding units for **1.XB**, **1.ChB** or **1.HB**, respectively; [b] *N* = 60000 frames, corresponding to 60 ns of sampling.

Table S5-3. Average intermolecular X···$^{-}O_2C$ distances[a,b] and C–X···$^{-}O_2C$ angles[a,b], along with corresponding standard deviations (SD), estimated from the concatenated molecular dynamics simulations of unbound and bound **1.XB**, **1.ChB** and **1.HB**.

Receptor	Anion	Scenario	X···$^{-}O_2C$ distances (Å)		C–X···$^{-}O_2C$ angles (°)	
			Avg ± SD	Range	Avg ± SD	Range
1.XB	Phthalate	A	2.841 ± 0.065	[2.619 ; 3.196]	173.5 ± 3.3	[153.7 ; 180.0]
			2.841 ± 0.065	[2.609 ; 3.195]	173.8 ± 3.2	[155.8 ; 180.0]
		B	2.843 ± 0.065	[2.604 ; 3.168]	174.1 ± 3.1	[152.5 ; 180.0]
			2.835 ± 0.064	[2.603 ; 3.134]	174.8 ± 2.8	[154.4 ; 180.0]
	Isophthalate	A	2.854 ± 0.065	[2.622 ; 3.328]	172.6 ± 3.7	[151.9 ; 180.0]
			2.847 ± 0.064	[2.616 ; 3.169]	173.4 ± 3.4	[149.3 ; 180.0]
		B	2.865 ± 0.076	[2.623 ; 3.332]	166.1 ± 6.8	[134.7 ; 179.9]
			2.867 ± 0.076	[2.612 ; 3.294]	165.9 ± 6.8	[129.5 ; 179.8]
	(*S*,*S*)-tartrate	B	2.866 ± 0.068	[2.631 ; 3.220]	170.4 ± 3.9	[146.9 ; 180.0]
			2.865 ± 0.068	[2.622 ; 3.216]	170.6 ± 3.9	[145.4 ; 180.0]
		C	2.960 ± 0.088	[2.696 ; 3.473]	157.2 ± 16.4	[99.4 ; 180.0]
			2.984 ± 0.089	[2.705 ; 3.614]	149.8 ± 17.4	[97.2 ; 179.9]
	(*R*,*R*)-tartrate	B	2.842 ± 0.064	[2.597 ; 3.212]	173.4 ± 3.4	[148.9 ; 180.0]
			2.843 ± 0.065	[2.597 ; 3.173]	173.4 ± 3.5	[151.4 ; 180.0]
		C	2.926 ± 0.067	[2.700 ; 3.355]	168.4 ± 5.2	[140.6 ; 180.0]
			2.926 ± 0.067	[2.700 ; 3.355]	168.3 ± 5.2	[141.3 ; 180.0]
1.ChB	Phthalate	A	2.958 ± 0.088	[2.630 ; 3.394]	164.5 ± 5.1	[138.4 ; 179.8]
			2.950 ± 0.088	[2.624 ; 3.358]	165.6 ± 4.9	[143.2 ; 179.8]
		B	2.945 ± 0.087	[2.565 ; 3.387]	166.0 ± 4.8	[140.2 ; 179.8]
			2.949 ± 0.086	[2.632 ; 3.347]	163.3 ± 4.5	[144.4 ; 179.8]
	Isophthalate	A	2.965 ± 0.085	[2.645 ; 3.372]	164.8 ± 5.5	[140.5 ; 179.9]
			2.986 ± 0.085	[2.676 ; 3.390]	162.1 ± 5.2	[138.4 ; 179.8]
		B	2.926 ± 0.084	[2.605 ; 3.317]	162.6 ± 4.9	[144.0 ; 179.8]
			2.928 ± 0.085	[2.615 ; 3.351]	162.3 ± 4.8	[142.8 ; 179.8]

[a)] X = I, Se or H binding units for **1.XB**, **1.ChB** or **1.HB**, respectively; [b)] *N* = 60000 frames, corresponding to 60 ns of sampling.

Table S5-3. Continued.

Receptor	Anion	Scenario	X···$^{-}$O$_2$C distances (Å)		C–X···$^{-}$O$_2$C angles (°)	
			Avg ± SD	Range	Avg ± SD	Range
1.ChB	(*S*,*S*)-tartrate	B	2.973 ± 0.087	[2.633 ; 3.416]	162.5 ± 4.9	[134.4 ; 178.9]
			2.973 ± 0.088	[2.646 ; 3.368]	162.8 ± 4.9	[128.3 ; 179.6]
		C	3.036 ± 0.092	[2.716 ; 3.465]	140.8 ± 21.0	[92.0 ; 179.9]
			3.039 ± 0.092	[2.721 ; 3.506]	139.5 ± 20.9	[88.4 ; 179.8]
	(*R*,*R*)-tartrate	B	2.973 ± 0.089	[2.663 ; 3.417]	162.3 ± 5.6	[111.3 ; 179.9]
			2.974 ± 0.089	[2.618 ; 3.399]	162.8 ± 5.3	[111.5 ; 179.8]
		C	2.993 ± 0.080	[2.692 ; 3.364]	161.9 ± 6.6	[119.0 ; 179.9]
			2.992 ± 0.080	[2.686 ; 3.398]	162.3 ± 6.4	[133.1 ; 179.9]
1.HB	Phthalate	A	2.178 ± 0.065	[1.954 ; 2.593]	138.9 ± 12.0	[105.6 ; 179.6]
			2.179 ± 0.065	[1.959 ; 2.522]	142.5 ± 11.6	[102.6 ; 179.0]
		B	2.183 ± 0.067	[1.950 ; 2.535]	139.6 ± 12.9	[102.1 ; 179.9]
			2.179 ± 0.066	[1.954 ; 2.537]	142.6 ± 12.9	[101.5 ; 179.6]
	Isophthalate	A	2.184 ± 0.067	[1.945 ; 2.660]	142.2 ± 11.1	[102.7 ; 179.5]
			2.182 ± 0.066	[1.959 ; 2.598]	142.0 ± 11.4	[101.2 ; 179.5]
		B	2.172 ± 0.065	[1.960 ; 2.533]	154.3 ± 11.9	[108.9 ; 180.0]
			2.171 ± 0.064	[1.945 ; 2.551]	155.2 ± 11.9	[106.2 ; 179.9]
	(*S*,*S*)-tartrate	B	2.180 ± 0.066	[1.961 ; 2.533]	143.7 ± 13.5	[102.6 ; 179.9]
			2.182 ± 0.067	[1.948 ; 2.549]	141.2 ± 14.3	[96.8 ; 179.8]
		C	2.215 ± 0.066	[1.999 ; 2.642]	135.9 ± 11.6	[99.4 ; 179.4]
			2.215 ± 0.066	[1.989 ; 2.687]	137.8 ± 11.9	[102.1 ; 179.7]
	(*R*,*R*)-tartrate	B	2.192 ± 0.068	[1.942 ; 2.572]	145.2 ± 8.9	[110.0 ; 179.4]
			2.194 ± 0.068	[1.964 ; 2.583]	145.3 ± 9.0	[108.0 ; 179.5]
		C	2.213 ± 0.065	[1.985 ; 2.626]	138.1 ± 12.7	[103.8 ; 179.9]
			2.211 ± 0.066	[1.990 ; 2.623]	144.6 ± 13.0	[105.4 ; 179.5]

[a] X = I, Se or H binding units for **1.XB**, **1.ChB** or **1.HB**, respectively; [b] *N* = 60000 frames, corresponding to 60 ns of sampling.

S5.3. Complete Molecular Modelling methods

Starting structures for chiral receptors, anion substrates and anion complexes

Starting structures of the chiral acyclic receptors **1.XB, 1.ChB** and **1.HB**, geometric anions phthalate and isophthalate, as well as enantiomeric anions (*S*,*S*)- and (*R*,*R*)-tartrate, were obtained from crystal structures deposited with the Cambridge Crystallographic Data Centre (CCDC).[5] The structures of phthalate and isophthalate were generated from NUTFIT[6] and BENZDC11[7] respectively. The structures of the (*S*,*S*)- and (*R*,*R*)-tartrates were obtained from AMHTAR02[8] and AHERAG,[9] respectively. The structure of the acyclic receptor **1.XB** was constructed using molecular fragments taken from the crystal structures with the following Refcodes: CUJTIM[10] (the two pyridinium-3,5-bis(iodotriazole) binding units) and VUTDIY[11] ((*S*)-1,1'-bi-2-naphthol (BINOL) central motif). These fragments were further linked affording the receptors' structure. **1.HB** and **1.ChB** structures were generated through appropriate atomic manipulation of **1.XB**, with the replacement of the iodine atoms with hydrogen ones and SeMe moieties, respectively.

Each aromatic dicarboxylate anion was then positioned in front of each receptor's binding units, being recognised by two putative cooperative bonding interactions to a single carboxylate (A) or to individual oxygen atoms of each carboxylate group (B). On the other hand, for the enantiomeric anions, an alternative scenario C, where each hydroxy oxygen atom is recognised by an independent binding unit, was considered instead of A.

Classical force field calculations

All Molecular Mechanics (MM) and Molecular Dynamics (MD) simulations were undertaken with Amber 2016 software suite.[12] The receptors and the oxyanions were described with default parameters taken from the Generalized Amber Force Field (GAFF)[13, 14] and RESP charges.[15] The force field parameters involving the selenium atoms were the same as previously developed for a Se-based macrocycle.[16] The hexafluorophosphate (PF_6^-) counter-ion was described with parameters and charges taken from ref. 17. The binary solvent mixture was described with the TIP3P model for the water molecules, while the acetone molecules were described with force field parameters taken from ref. 18.

Calculation of RESP charges

The RESP charges derivatisation of the three receptors consisted of molecular geometry optimizations with the B3LYP functional along with 6-31G(d) basis set, followed by the calculation of the electrostatic potential through a single point carried out at the HF/6-31G(d) theory level, using 4 concentric surface layers and 6 points per layer, in agreement with GAFF development.[13, 14] In addition, the iodine atoms of **1.XB** and the selenium atoms of **1.ChB** were described with the aug-cc-pVDZ-PP and the aug-cc-pVDZ basis sets, respectively, obtained from the EMSL database.[19, 20] The dicarboxylate anions were optimised at the B3LYP/6-31+G(d,p) theory level, followed by electrostatic potential calculation, as stated above. The atomic charges of the (*S*,*S*)-tartrate were used for both enantiomers. All these quantum calculations were carried out with the Gaussian 09 software.[21]

Modelling of XB and ChB interactions

The XB and ChB interactions were described with resort to an extra-point (EP) of charge[22] with van der Waals parameters and mass set to zero. In **1.XB**, an extra-point was bonded to each iodine triazole binding site by the use of an I-EP distance of 1.99 Å, with a bond stretching force constant of 600 kcal·mol^{-1}·Å^{-2} and C-I-EP angle of 180°, with an angle bending force constant of 150 kcal·mol^{-1}·rad^{-2}. This I-EP optimal distance was previously found to described XB interactions between carboxylate anions and iodotriazolium activated binding sites.[23-25] On the other hand, in **1.ChB**, the extra-points were bonded to the selenotriazolium binding sites by the use of an Se-EP distance of 1.99 Å, a bond stretching force constant of 600 kcal·mol^{-1}·Å^{-2} and $C_{triazolium}$-Se-EP and C_{methyl}-Se-EP angles of 166 and 67°, respectively, with angle bending force constants of 150 kcal·mol^{-1}·rad^{-2}, as previously established.[16] Table S5-4 lists the RESP charges calculated for the EP, and for the iodine and selenium atoms in **1.XB** and **1.ChB**, respectively, both with and without the EP.

Table S5-4. EP, iodine and selenium RESP charges (*q*(e)) derivatised for I/Se-EP distance of 1.99 Å.

I/Se-EP distance (Å)	**1.XB**		**1.ChB**	
	EP	I	EP	Se
1.99	0.090737	-0.025744	0.079672	-0.172079
No EP	-	0.266118	-	-0.012386

*DFT optimisations of free **1.XB$_{Me}$** and **1.ChB$_{Me}$** models, geometric dicarboxylates, (S,S)-tartrate, and model complexes with isophthalate (B)*

Preliminary characterisation of the binding ability of model receptors **1.XB$_{Me}$** and **1.ChB$_{Me}$**, in which the flexible octyl chains of **1.XB** and **1.ChB** were replaced with methyl groups, was ascertained via DFT calculations. TeraChem[26-30] was employed to optimise the ground state gas-phase structures of the two model receptors, employing the ωB97X functional and the 6-311++G(d,p) basis set for all atoms apart I (aug-cc-pVDZ-PP) and Se (aug-cc-pVDZ). The phthalate, isophthalate, and (*S*,*S*)-tartrate anions were also optimised at the same theory level. These structures were found to be at minima due to the absence of negative frequencies in the vibrational frequencies calculated using DFT. Furthermore, from these DFT optimised structures, the distribution of the electrostatic potential (*V*) mapped onto the electron density surface of **1.XB$_{Me}$** and **1.ChB$_{Me}$** (V_S), as well as of the anions, was ascertained using MultiWFN,[31, 32] and is presented in Figure 5-2 (receptors) and S5-1 (anions).

In our previous studies,[16, 23-25] we have shown that the recognition of anionic guests by XB or ChB interactions in aqueous organic solvent mixture occurs concomitantly with the I/Se binding sites being preferentially solvated by water molecules. Based on this structural feature, the XB, ChB and HB dimensions were gauged in the isophthalate complexes of **1.XB$_{Me}$**, **1.ChB$_{Me}$** and **1.HB$_{Me}$** complexes in scenario B (see above), *via* DFT optimisations with the electrostatic interactions between the complexes and continuum model of water being described using the conductor-like screening model (COSMO),[33] and a dielectric constant ε of 78.3553.[34] The DFT optimisations were carried out at the same theory level of the corresponding free models. The dimensions of the XB and ChB interactions in the DFT optimised structures are summarised in Table S5-5 and were further used to establish the distance and angle restraints employed in the MD simulations of **1.XB**, **1.ChB** and **1.HB$_{Me}$** anion complexes in solution.

Table S5-5. Dimensions of the XB and ChB interactions of **1.XB$_{Me}$** and **1.ChB$_{Me}$** with isophthalate in scenario B from DFT optimisations using the COSMO solvation model for water.

Receptor	$z\cdots O_2C^-$ distances (Å)[a]	$C–z\cdots O_2C^-$ angles (°)[a]
1.XB	2.73 ; 2.76	164.2 ; 161.0
1.ChB	2.88 ; 2.96	163.4 ; 155.9

[a] z = I or Se for **1.XB$_{Me}$** or **1.ChB$_{Me}$**, respectively.

General MD simulation methods

Preliminary MD simulations, both in gas-phase and in solution (not reported), have shown that the XB bonding interactions alone were insufficient to maintain the stability of the oxyanion complexes of **1.XB**. Thus, the synergetic XB, ChB and HB interactions between the oxygen atoms of the carboxylate groups and the C–I/C–Se/ C–H binding units were maintained roughly linear by the application of suitable $z\cdots O$ distance restraints complemented by angle restraints on the C-$z\cdots O$ angles, based on the previous DFT optimised structures of the isophthalate complexes described above.

These distance and angle restraints employed in MM gas-phase minimisations of the **1.XB**, **1.ChB** and **1.HB** complexes. Afterwards, the structures obtained in gas phase were solvated with Packmol[35] in cubic boxes composed of 627 water molecules and 871 acetone molecules, randomly distributed, corresponding to the binary solvent mixture of acetone/water 85:15 v/v used in the ^{1}H NMR binding studies.

Each oxyanion complex was equilibrated under periodic boundary conditions using the following multi-stage protocol. The system was relaxed by MM minimization of the solvent molecules and by keeping the solute fixed with a strong positional restraint of 500 kcal mol^{-1} Å^{-2}. The positional restraint was then removed and the entire system was minimized only with the distance and angle restraints. Both minimization stages comprised an initial set of 10000 steepest descent algorithm steps, followed by 10000 steps of conjugated gradient algorithm. The equilibration stage proceeded heating up the system to 300 K for 100 ps using a NVT ensemble and a weak positional restraint (10 kcal mol^{-1} Å^{-2}) on the solutes. Subsequently the density of the system was adjusted using a NPT ensemble at 300 K and 1 atm for 1 ns. This simulation protocol ended with a NPT data collection run carried out for 20 ns, with trajectory frames being saved every 1 ps. In both NPT stages, distance and angle restraints with suitable force constants were employed to assure the stability of the oxyanion complexes. Three independent runs were performed for each anion binding complex. The free receptors, in the presence of two noncoordinating PF_6^- counter-ions, were simulated with the same equilibration protocol, asunder of the distance and angle restraints, also in three independent MD runs. The CUDA version of the PMEMD executable was used for the simulation of all solvated systems.[36, 37] The bond lengths involving all bonds to hydrogen atoms were constrained with the SHAKE algorithm allowing the usage of 2 fs time step.[38] The Particle Mesh Ewald (PME) method was used to treat the long-range electrostatic interactions.[39] The non-bonded van der Waals interactions were truncated with a 10 Å cut-off. The structural data were calculated for a total sampling time of 60 ns by post-processing the trajectory files of three independent MD runs with *cpptraj*.[40]

S6. References

1. B.-Y. Lee, S. R. Park, H. B. Jeon and K. S. Kim, *Tetrahedron Lett.*, 2006, **47**, 5105–5109.
2. Y. Takeda, M. Okazaki and S. Minakata, *Chem Commun*, 2014, **50**, 10291–10294.
3. *www.supramolecular.org*, .
4. M. J. Hynes, *J. Chem. Soc. Dalton Trans.*, 1993, 311–312.
5. C. R. Groom, I. J. Bruno, M. P. Lightfoot and S. C. Ward, *Acta Crystallogr B Struct Sci Cryst Eng Mater*, 2016, **72**, 171-179.
6. P. Sahoo, N. N. Adarsh, G. E. Chacko, S. R. Raghavan, V. G. Puranik and P. Dastidar, *Langmuir*, 2009, **25**, 8742-8750.
7. F. R. Fronczek, *CSD Communication*, 2015, DOI: 10.5517/cc1j9yc4.
8. L.R.Falvello, *CSD Communication*, 2014, DOI: 10.5517/cc57lhg.
9. K. Rajagopal, M. S. Nandhini, R. V. Krishnakumar and S. Natarajan, *Acta Crystallogr E*, 2002, **58**, O1306-O1308.
10. S. W. Robinson, C. L. Mustoe, N. G. White, A. Brown, A. L. Thompson, P. Kennepohl and P. D. Beer, *J. Am. Chem. Soc.*, 2015, **137**, 499-507.
11. C. Coluccini, D. Dondi, M. Caricato, A. Taglietti, M. Boiocchi and D. Pasini, *Org Biomol Chem*, 2010, **8**, 1640-1649.
12. D. A. Case, R. M. Betz, W. Botello-Smith, D. S. Cerutti, T. E. Cheatham, 3rd, T. A. Darden, R. E. Duke, T. J. Giese, H. Gohlke, A. W. Goetz, N. Homeyer, S. Izadi, P. Janowski, J. Kaus, A. Kovalenko, T. S. Lee, S. LeGrand, P. Li, C. Lin, T. Luchko, R. Luo, B. Madej, D. Mermelstein, K. M. Merz, G. Monard, H. Nguyen, H. T. Nguyen, I. Omelyan, A. Onufriev, D. R. Roe, A. Roitberg, C. Sagui, C. L. Simmerling, J. Swails, R. C. Walker, J. Wang, R. M. Wolf, X. Wu, L. Xiao, D. M. York and P. A. Kollman, *Journal*, 2016.
13. J. Wang, R. M. Wolf, J. W. Caldwell, P. A. Kollman and D. A. Case, *J. Comput. Chem.*, 2004, **25**, 1157-1174.
14. J. Wang, R. M. Wolf, J. W. Caldwell, P. A. Kollman and D. A. Case, *J. Comput. Chem.*, 2005, **26**, 114-114.
15. C. I. Bayly, P. Cieplak, W. D. Cornell and P. A. Kollman, *J. Phys. Chem.*, 1993, **97**, 10269-10280.
16. J. Y. Lim, I. Marques, A. L. Thompson, K. E. Christensen, V. Felix and P. D. Beer, *J. Am. Chem. Soc.*, 2017, **139**, 3122-3133.
17. Z. P. Liu, S. P. Huang and W. C. Wang, *J. Phys. Chem. B*, 2004, **108**, 12978-12989.
18. S. K. Burger and G. A. Cisneros, *J. Comput. Chem.*, 2013, **34**, 2313-2319.
19. D. Feller, *J. Comput. Chem.*, 1996, **17**, 1571-1586.
20. K. L. Schuchardt, B. T. Didier, T. Elsethagen, L. Sun, V. Gurumoorthi, J. Chase, J. Li and T. L. Windus, *J. Chem. Inf. Model.*, 2007, **47**, 1045-1052.
21. M. J. Frisch, G. W. Trucks, H. B. Schlegel, G. E. Scuseria, M. A. Robb, J. R. Cheeseman, G. Scalmani, V. Barone, B. Mennucci, G. A. Petersson, H. Nakatsuji, M. Caricato, X. Li, H. P. Hratchian, A. F. Izmaylov, J. Bloino, G. Zheng, J. L. Sonnenberg, M. Hada, M. Ehara, K. Toyota, R. Fukuda, J. Hasegawa, M. Ishida, T. Nakajima, Y. Honda, O. Kitao, H. Nakai, T. Vreven, J. J. A. Montgomery, J. E. Peralta, F. Ogliaro, M. Bearpark, J. J. Heyd, E. Brothers, K. N. Kudin, V. N. Staroverov, R. Kobayashi, J. Normand, K. Raghavachari, A. Rendell, J. C. Burant, S. S. Iyengar, J. Tomasi, M. Cossi, N. Rega, J. M. Millam, M. Klene, J. E. Knox, J. B. Cross, V. Bakken, C. Adamo, J. Jaramillo, R. Gomperts, R. E. Stratmann, O. Yazyev, A. J. Austin, R. Cammi, C. Pomelli, J. W. Ochterski, R. L. Martin, K. Morokuma, V. G. Zakrzewski, G. A. Voth, P. Salvador, J. J. Dannenberg, S. Dapprich, A. D. Daniels, Ö. Farkas, J. B. Foresman, J. V. Ortiz, J. Cioslowski and D. J. Fox, *Journal*, 2009.
22. M. A. Ibrahim, *J. Comput. Chem.*, 2011, **32**, 2564-2574.
23. J. Y. Lim, I. Marques, L. Ferreira, V. Felix and P. D. Beer, *Chem. Commun.*, 2016, **52**, 5527-5530.
24. J. Y. C. Lim, I. Marques, V. Felix and P. D. Beer, *J. Am. Chem. Soc.*, 2017, **139**, 12228-12239.
25. J. Y. C. Lim, I. Marques, V. Felix and P. D. Beer, *Angew. Chem. Int. Ed. Engl.*, 2018, **57**, 584-588.
26. I. S. Ufimtsev and T. J. Martinez, *J. Chem. Theory Comput.*, 2009, **5**, 2619-2628.
27. A. V. Titov, I. S. Ufimtsev, N. Luehr and T. J. Martinez, *J. Chem. Theory Comput.*, 2013, **9**, 213-221.
28. C. Song, L. P. Wang and T. J. Martinez, *J. Chem. Theory Comput.*, 2016, **12**, 92-106.

29. J. Kastner, J. M. Carr, T. W. Keal, W. Thiel, A. Wander and P. Sherwood, *J. Phys. Chem. A*, 2009, **113**, 11856-11865.
30. T. P. Goumans, C. R. Catlow, W. A. Brown, J. Kastner and P. Sherwood, *Phys. Chem. Chem. Phys.*, 2009, **11**, 5431-5436.
31. T. Lu and F. Chen, *J. Comput. Chem.*, 2012, **33**, 580-592.
32. T. Lu and F. Chen, *J. Mol. Graph. Model.*, 2012, **38**, 314-323.
33. F. Liu, N. Luehr, H. J. Kulik and T. J. Martinez, *J. Chem. Theory Comput.*, 2015, **11**, 3131-3144.
34. J. J. C. Teixeira-Dias, in *Molecular Physical Chemistry*, ed. J. J. C. Teixeira-Dias, Springer International Publishing, Cham, 2017, DOI: 10.1007/978-3-319-41093-7_7, ch. Chapter 7, pp. 331-398.
35. L. Martinez, R. Andrade, E. G. Birgin and J. M. Martinez, *J. Comput. Chem.*, 2009, **30**, 2157-2164.
36. S. Le Grand, A. W. Götz and R. C. Walker, *Comput. Phys. Commun.*, 2013, **184**, 374-380.
37. R. Salomon-Ferrer, A. W. Gotz, D. Poole, S. Le Grand and R. C. Walker, *J. Chem. Theory Comput.*, 2013, **9**, 3878-3888.
38. J.-P. Ryckaert, G. Ciccotti and H. J. C. Berendsen, *J. Comput. Phys.*, 1977, **23**, 327-341.
39. T. Darden, D. York and L. Pedersen, *J. Chem. Phys.*, 1993, **98**, 10089-10092.
40. D. R. Roe and T. E. Cheatham, 3rd, *J. Chem. Theory Comput.*, 2013, **9**, 3084-3095.